



# Chemical Synthesis and Applications of Colloidal Metal Phosphide Nanocrystals

Hui Li<sup>1</sup>, Chao Jia<sup>1</sup>, Xianwei Meng<sup>2</sup> and Hongbo Li<sup>1\*</sup>

<sup>1</sup> Beijing Key Laboratory of Construction-Tailorable Advanced Functional Materials and Green Applications, School of Materials Science & Engineering, Beijing Institute of Technology, Beijing, China, <sup>2</sup> Laboratory of Controllable Preparation and Application of Nanomaterials, CAS Key Laboratory of Cryogenics, Technical Institute of Physics and Chemistry, Chinese Academy of Sciences, Beijing, China

## OPEN ACCESS

### Edited by:

Vladimir Lesnyak,  
Technische Universität Dresden,  
Germany

### Reviewed by:

Sergey V. Gaponenko,  
BI Stepanov Institute of Physics  
(NASB), Belarus  
Zhenmeng Peng,  
University of Akron, United States

### \*Correspondence:

Hongbo Li  
hbli@mail.ipc.ac.cn

### Specialty section:

This article was submitted to  
Nanoscience,  
a section of the journal  
Frontiers in Chemistry

Received: 28 September 2018

Accepted: 13 December 2018

Published: 08 January 2019

### Citation:

Li H, Jia C, Meng X and Li H (2019)  
Chemical Synthesis and Applications  
of Colloidal Metal Phosphide  
Nanocrystals. *Front. Chem.* 6:652.  
doi: 10.3389/fchem.2018.00652

Colloidal nanocrystals (NCs) have emerged as promising materials in optoelectronic devices and biological imaging application due to their tailorable properties through size, shape, and composition. Among these NCs, metal phosphide is an important class, in parallel with metal chalcogenide. In this review, we summarize the recent progress regarding the chemical synthesis and applications of colloidal metal phosphide NCs. As the most important metal phosphide NCs, indium phosphide (InP) NCs have been intensively investigated because of their low toxicity, wide and tunable emission range from visible to the near-infrared region. Firstly, we give a brief overview of synthetic strategies to InP NCs, highlighting the benefit of employing zinc precursors as reaction additive and the importance of different phosphorus precursors to improve the quality of the InP NCs, in terms of size distribution, quantum yield, colloidal stability, and non-blinking behavior. Next, we discuss additional synthetic techniques to overcome the issues of lattice mismatch in the synthesis of core/shell metal phosphide NCs, by constructing an intermediate layer between core/shell or designing a shell with gradient composition in a radial direction. We also envision future research directions of InP NCs. The chemical synthesis of other metal phosphide NCs, such as II-V metal phosphide NCs ( $\text{Cd}_3\text{P}_2$ ,  $\text{Zn}_3\text{P}_2$ ) and transition metal phosphides NCs ( $\text{Cu}_3\text{P}$ ,  $\text{FeP}$ ) is subsequently introduced. We finally discuss the potential applications of colloidal metal phosphide NCs in photovoltaics, light-emitting diodes, and lithium ion battery. An overview of several key applications based on colloidal metal phosphide NCs is provided at the end.

**Keywords:** colloidal nanocrystals, indium phosphide, phosphorus precursors, II-V metal phosphide nanocrystals, transition metal phosphides nanocrystals

## INTRODUCTION

Colloidal nanocrystals (NCs) that exhibit unique optical and electrical properties have attracted considerable attention due to diverse applications such as photovoltaics, optoelectronics, (Coe et al., 2002; Dai et al., 2014; Pietryga et al., 2016; Panfil et al., 2018), and biomedical imaging (Michalet et al., 2005; Hong et al., 2017). Among these NCs, metal phosphide NCs are chemical compounds containing phosphorus and one or more metals, with formula of  $\text{M}_x\text{P}_y$ . Phosphorus is known to be able to form at least one stable compounds (e.g., InP,  $\text{Cu}_3\text{P}$ ) with d-group metals and most of the rare earth metals. Besides, many metal phosphides have multiple stoichiometry,

providing various crystal structures for binary metal phosphides. Most of the metal phosphide NCs share metal–metalloid bonds (M–P) with a strong covalent component (Greenwood et al., 1966). These bonds are often combined with highly covalent metalloid–metalloid bonds (P–P) (Carenco et al., 2013), where the formation of covalent bond requires harsher reaction conditions for the colloidal chemical synthesis, such as highly active precursors or high reaction temperature. Unlike the metal chalcogenide, metal phosphide can be semiconductors, insulators, and conductors, which are highly dependent on the chemical composition, crystal structure, and electronic state. These specific features provide metal phosphides with unique properties, and also facilitate many potential applications.

Nowadays, conventional cadmium and lead based NCs have been judged because of environmental concerns on heavy metals. Therefore, InP NCs present an attractive alternative owing to low toxicity and emission tunability ranging from visible to near-infrared region (Ramasamy et al., 2017). Zinc phosphide ( $\text{Zn}_3\text{P}_2$ ) is an intriguing material for photovoltaic (Luber et al., 2013). It has a band gap of 1.5 eV, a large absorption coefficient, a long minority-carrier diffusion length. Transition metal phosphides also have great potential in energy conversion and storage applications.

To synthesize colloidal NCs, cationic, and anionic precursors are indispensable with ligands, non-coordinating solvent as well as high temperature exposure to advance reaction. As for anion precursors in metal phosphide NCs, phosphorus precursors that have been used in the colloidal synthesis can be classified into different types, including the single source precursor ( $\text{In}(\text{PBU}_2)_3$ ) (Green and O'Brien, 1998),  $\text{P}(\text{SiMe}_3)_3$ , metal phosphorus ( $\text{Na}_3\text{P}$ ) (Jun et al., 2006), magic sized clusters (MSCs) (Friedfeld et al., 2017), elemental phosphorus precursor (Ung et al., 2008; Bang et al., 2017), and  $\text{PH}_3$  gas (Zan and Ren, 2012). **Figure 1** shows different types of phosphorus precursors that have been applied in the chemical synthesis of metal phosphide NCs. Regardless of investigations of various phosphorus precursors,  $\text{P}(\text{SiMe}_3)_3$  tend to obtain high quality of InP NCs. However, air and water-free conditions are necessary for the sensitive, hazardous nature of  $\text{P}(\text{SiMe}_3)_3$ . In addition, scalability is also a crucial factor because of the demand of large quantity of NCs in commercial applications. In this case, aminophosphine precursors are found to give access to NCs with comparable characteristics as  $\text{P}(\text{SiMe}_3)_3$ . In the following sections, the reaction mechanism of InP formation with aminophosphine precursors will be summarized. Several colloidal syntheses utilize TOP and  $\text{P}(\text{SiMe}_3)_3$  to obtain zinc phosphide and transition metal phosphides NCs, which borrow experiences from other metal phosphide NCs (Luber et al., 2013; Ramasamy et al., 2017).

The undercoordinated surface atoms in NC surfaces, acting as trap states, will affect the lifetime, efficiency of electron hole pairs, radiative recombination. Coating an additional shell provides extra means to manipulate the properties. Typically, type I core/shell NCs feature a strongly enhanced photoluminescence quantum yield (PLQY), such as InP/ZnS, and InP/ZnSe. Moreover, insert buffer layers (InP/GaP/ZnS) or adjust the lattice constant of core and shell (InZnP/ZnSeS) can minimize strain

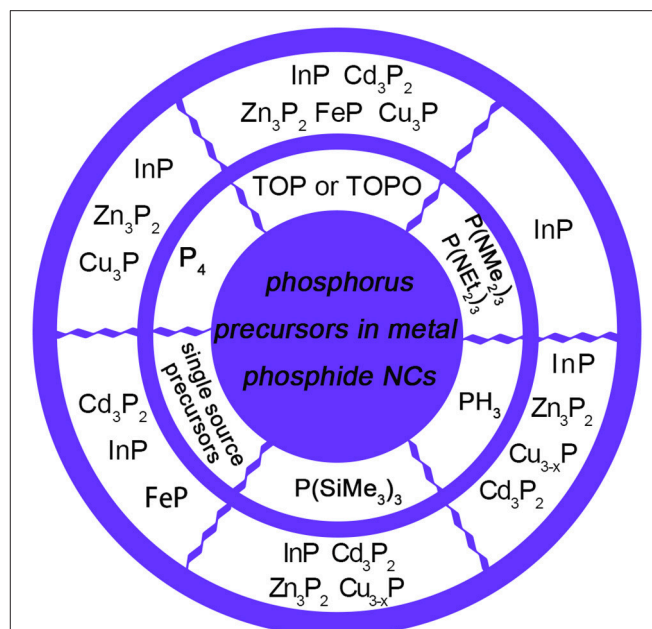


**FIGURE 1** | Various types of phosphorus precursors used in the synthesis of metal phosphide NCs. InP NCs could be synthesized by TOP (Lauth et al., 2013),  $\text{P}(\text{NMe}_2)_3$  (Song et al., 2013),  $\text{P}(\text{NEt}_2)_3$  (Tessier et al., 2015),  $\text{PH}_3$  (Li et al., 2008),  $\text{P}(\text{SiMe}_3)_3$  (Micic et al., 1994),  $\text{P}_4$  (Ung et al., 2008), and single source precursors, including  $\text{In}(\text{PBU}_2)_3$  (Green and O'Brien, 1998) and magic-size clusters (MSCs) (Gary et al., 2015).  $\text{Zn}_3\text{P}_2$  NCs could be synthesized by TOP (Mobarok et al., 2014),  $\text{PH}_3$  (Miao et al., 2013),  $\text{P}(\text{SiMe}_3)_3$  (Ho et al., 2015), and  $\text{P}_4$  (Carenco et al., 2010).  $\text{Cd}_3\text{P}_2$  NCs could be synthesized by TOP (Khanna et al., 2010),  $\text{PH}_3$  (Miao et al., 2012),  $\text{P}(\text{SiMe}_3)_3$  (Miao et al., 2010), and MSCs (Li et al., 2014) acting as single source precursors. FeP could be synthesized by TOP (Henkes and Schaak, 2007) and  $(\text{CO})_4\text{Fe}(\text{PH}_3)$  (Hunger et al., 2013) acting as single source precursors. Copper phosphides could be synthesized by TOP (Henkes and Schaak, 2007),  $\text{PH}_3$  (Manna et al., 2013),  $\text{P}(\text{SiMe}_3)_3$  (Liu et al., 2016), and  $\text{P}_4$  (Bichat et al., 2004a).

and alleviate interfacial defects, which is resulted from lattice mismatch in core/shell NCs.

In this review, a representative introduction on the physical properties of metal phosphide NCs is given firstly. Selecting suitable precursor plays an important role in the chemical synthesis of NCs. Different from the synthesis of metal chalcogenide, much more phosphorus precursors have been tested with the purpose of improving the quality, and reducing the production cost of metal phosphide NCs. We give a detail discussion regarding the underlying chemical mechanism on the phosphorus chemistry in the synthesis of metal phosphide NCs. As one key example of metal phosphide, strategies to obtain high quality InP NCs and their core/shell system with ZnS and ZnSe as passivating shells are summarized. A passivating shell is of critical importance for InP NCs, because their surfaces are prone to be easily oxidized. We also conclude by pointing out challenges to be addressed in future research, such as broad emission, shape control, and doping of InP NCs. Next, II-V metal phosphide NCs (e.g.,  $\text{Cd}_3\text{P}_2$ ,  $\text{Zn}_3\text{P}_2$ ) and transition metal phosphides (e.g., copper phosphide, iron phosphide) are presented. Finally, an overview of state-of-the-art applications

with metal phosphide NCs is provided, such as light-emitting devices (LEDs), photovoltaic cells, and biomedical applications.

## PHOSPHORUS PRECURSORS IN COLLOIDAL SYNTHESIS OF INP NANOCRYSTALS

As the most important metal phosphide, InP has attracted intensive attention. (Green and O'Brien, 1998; Jun et al., 2006; Ung et al., 2008; Zan and Ren, 2012; Bang et al., 2017; Friedfeld et al., 2017). The direct band gap of 1.35 eV, high fraction of covalent bonding and the large Bohr exciton radius of 9.6 nm make the InP NCs an excellent candidate as visible and near-IR emitting materials. The first liquid colloidal synthesis of InP NCs with narrow size distribution was realized by Nozik in 1994 by using  $P(\text{SiMe}_3)_3$  (Micic et al., 1994). The P–Si bond in the compound of  $P(\text{SiMe}_3)_3$  exhibits relatively low dissociation energy (around  $363 \text{ kJ mol}^{-1}$ ), which leads to its high reactivity in the case of reacting with an indium precursor. Besides, the phosphorus atom bonded to the highly electropositive Si atom imparts the necessary driving force to react with indium precursors. Therefore, the resulting InP NCs show well-crystallized zinc blende structure and modest exciton peak attributed to InP, which is the first time to show an exciton peak for an III-V NC. This strategy was also applied to the synthesis of other binary and ternary III-V QDs, e.g., GaP, GaInP<sub>2</sub> (Micic et al., 1995). Since this pioneering report,  $P(\text{SiMe}_3)_3$  has become the most widely used phosphorus precursor in the colloidal synthesis of metal phosphide NCs. Then, utilizing  $P(\text{SiMe}_3)_3$  precursor, Micic et al. treated the NCs with a solution of HF or  $\text{NH}_4\text{F}$ , resulting in highly efficient band-edge emission (Micic et al., 1996, 1997).

In view of their highly reactivity,  $P(\text{SiMe}_3)_3$  will be consumed in a few seconds. In this context, the growth of NCs tends to proceed via the Ostwald ripening mechanism, which widens the size distribution (Clark et al., 2011). Furthermore, due to pyrophoric nature, high cost, and hazardous reagents of  $P(\text{SiMe}_3)_3$  and secondary products involved in production, several alternatives for  $P(\text{SiMe}_3)_3$  are already studied (Reiss et al., 2016). Up to now, following the first synthesis of InP NCs, a variety of phosphorus precursors have been investigated with the main purpose of improving the size distribution. A diversity of phosphorus precursors in the synthesis of InP NCs is summarized in **Table 1**.

Similar to  $P(\text{SiMe}_3)_3$  precursor, single-source precursor is a highly reactive precursor, which can shorten the reaction time and avoid the formation of side products, such as of  $\text{In}_2\text{O}_3$ . Mark et al. reported the synthesis of high quality InP NCs by using the single source precursor of  $(\text{In}(\text{PBU}_2)_3)$  (Green and O'Brien, 1998). It is noted that the preparation and storage of such a highly reactive precursor requires great cautions. To address these issues, Li et al. synthesized high quality InP NCs by using the *in situ* generated  $\text{PH}_3$  gas as the phosphorus precursor (Li et al., 2008; Zan and Ren, 2012).  $\text{PH}_3$  is a more stable and safer phosphorus precursor, compared to pyrophoric  $P(\text{SiMe}_3)_3$  precursor. Furthermore, the method based on  $\text{PH}_3$

gas gives access to larger sized InP NCs. In 2008, Reiss et al. reported the synthesis of InP NCs using an elemental P precursor (red P allotropes) as the phosphorus precursor. To stimulate the reaction,  $\text{NaBH}_4$  was introduced as the reducing agent. The reaction could proceed with a very high reaction yield approaching 100% (Ung et al., 2008). Park et al. reported the synthesis of highly luminescent InP/ZnS NCs using an elemental P precursor of  $\text{P}_4$  (white P) (Bang et al., 2017). They demonstrated that the direct reaction of  $\text{P}_4$  precursor with In precursor without reducing agent. The sublimation of red P powder can simply produce  $\text{P}_4$ , therefore  $\text{P}_4$  precursor represents an additional low-cost P precursor and provides an important way to the large-scale synthesis on InP NCs.

In order to avoid the rapid depletion of  $P(\text{SiMe}_3)_3$ , phosphorus precursors with decreased precursor reactivity have been synthesized. Different strategies have been implemented, such as replacing the Si with Ge or Sn (Harris and Bawendi, 2012), substituting methyl group with butyl or aryl group (Joung et al., 2012; Gary et al., 2014). Replacing Si in the Si–P bond with Ge or Sn reduces the reactivity of the precursor by decreasing the polarity of the bond. Likewise, altering the methyl groups to sterically hindering moieties can reduce the reactivity as well. It is believed that using less reactive precursor is helpful to segregate the nucleation and growth and is essential to reach InP NCs with narrow size distribution. Despite great efforts, these alternatives exhibited either largely unchanged or very slowed conversions compared with  $P(\text{SiMe}_3)_3$ .

Aminophosphine presents an alternative phosphorus precursor with advantages of low cost, high stability, decent reactivity, and easy handling (Xie et al., 2007; Laufersky et al., 2018; Mundy et al., 2018). Song and coworkers reported for the first time of high-quality InP NCs using  $P(\text{NMe}_2)_3$  as a phosphorus precursor (Song et al., 2013). The synthesis was performed by rapid injection of  $P(\text{NMe}_2)_3$  into the  $\text{InCl}_3$  and  $\text{ZnCl}_2$  solution with oleylamine at  $220^\circ\text{C}$ . They found that the size and size distributions of InP NCs are depended on the amount of  $P(\text{NMe}_2)_3$ ,  $\text{ZnCl}_2$  as well as the growth temperature and time. The presence of  $\text{ZnCl}_2$  in the synthesis plays a role in activating the aminophosphine to undergo a disproportionation reaction and form  $\text{P}^{3-}$ , which is helpful to achieve narrow size distribution (Laufersky et al., 2018).

Later, Tessier presented an investigation into the chemical reactions of InP formation with  $\text{InCl}_3$  and aminophosphine precursors (Tessier et al., 2016). Using NMR spectroscopy and single crystal X-ray diffraction and mass spectrometry, they demonstrated that the InP formation underwent  $4\text{P}(+\text{III}) \rightarrow \text{P}(-\text{III}) + 3\text{P}(+\text{V})$  disproportionation reaction. Since aminophosphines are P(III) compounds, reduction steps are needed to form InP with an In (III) precursor. As shown in **Scheme 1A**, an exchange between primary amines and amino groups of phosphorus precursor occurs, indicating that apart from acting as solvent or ligand, primary amines also play an important role in the whole precursor chemistry. Then, 1 equiv of InP is formed by oxidating 3 equiv of the substituted aminophosphine to a phosphonium salt (**Scheme 1B**). Namely, substituted aminophosphine has a double role in the reaction, both phosphorus precursor and reducing agent. Based on double

**TABLE 1** | Summary of phosphorus precursors in colloidal synthesis of InP NCs.

	<b>P precursors</b>	<b>In precursors</b>	<b>Methods</b>	<b>Results</b>	<b>References</b>
1998	In(PBu <sub>2</sub> <sup>t</sup> ) <sub>3</sub>		Decomposition of In(PBu <sub>2</sub> <sup>t</sup> ) <sub>3</sub>	Quantum confinement effects	Green and O'Brien, 1998
2006	Na <sub>3</sub> P	InCl <sub>3</sub>	Heat-up	Spherical NCs with 5 nm	Jun et al., 2006
2008	P <sub>4</sub>	InCl <sub>3</sub>	Hot-injection	Cubic structure with 3–4 nm	Ung et al., 2008
2008	PCl <sub>3</sub>	In(Ac) <sub>3</sub>	Heat-up	Size tunability; HF-etching improved the quantum yield (QY)	Liu et al., 2008
2008, 2012	PH <sub>3</sub>	In(Ac) <sub>3</sub>	Gas-liquid phase synthesis	InP/ZnS NCs: QY of 30–60%	Li et al., 2008; Zan and Ren, 2012
2012	P(SiMe <sub>2</sub> -tert-Bu) <sub>3</sub>	In(Ac) <sub>3</sub>	Hot-injection	Large size of InP NCs: InP/ZnS NCs: QY of 18–28%	Joung et al., 2012
2012	P(GeMe <sub>3</sub> ) <sub>3</sub>	In(MA) <sub>3</sub>	Hot-injection	Improved size distribution	Harris and Bawendi, 2012
2013	P(NMe <sub>2</sub> ) <sub>3</sub>	InCl <sub>3</sub>	Hot-injection	Size tunability; InP/ZnS NCs: emission FWHM:60–64 nm; QY: 51–53%	Song et al., 2013
2013	TOP	InCl <sub>3</sub> , InF <sub>3</sub> , InBr <sub>3</sub>	Hot-injection	Size tunability	Lauth et al., 2013
2014	P(SiPh <sub>3</sub> ) <sub>3</sub> , P(SiMe <sub>3</sub> ) <sub>3</sub>	In(MA) <sub>3</sub>	Hot-injection	Separated the nucleation and growth	Gary et al., 2014
2015	Single-source precursors: InP MA MSCs from P(SiMe <sub>3</sub> ) <sub>3</sub> and In(MA) <sub>3</sub>		Hot-injection	Conversion of InP MSCs to NCs proceeded via a supersaturated solution	Gary et al., 2015
2015	P(NEt <sub>2</sub> ) <sub>3</sub>	InCl <sub>3</sub> , InI <sub>3</sub> , InBr <sub>3</sub>	Hot-injection	InP/ZnS NCs: emission FWHM of 46–63 nm; QY: 50–60%	Tessier et al., 2015
2017	P(SiMe <sub>3</sub> ) <sub>3</sub>	In(Ac) <sub>3</sub>	Heat-up	Zn–P intermediate complex lowered the reactivity of P(SiMe <sub>3</sub> ) <sub>3</sub>	Koh et al., 2017
2017	P <sub>4</sub>	InCl <sub>3</sub> , InI <sub>3</sub>	Hot-injection	Large-scale production; InP/ZnS NCs: emission FWHM: 50–80 nm; QY: 60%	Bang et al., 2017

role of phosphorus, this mechanism assumes a nucleophilic attack by the phosphorus center of one aminophosphine on an amino group of another aminophosphine. Firstly, InCl<sub>3</sub> reacts with P(NHR)<sub>3</sub> to form adducts with different resonance structures (**Scheme 1B-I**), thus, the positive charge can delocalize over the phosphorus center and the nitrogen atoms, making it possible for residual P(NHR)<sub>3</sub> to nucleophilic attack nitrogen atoms, as showed in **Scheme 1B-II**. Subsequent phosphorus nucleophilic substitution results in InP unit formation. This mechanism explains why full conversion of the In precursor is only attained for a 4:1 P/In ratio.

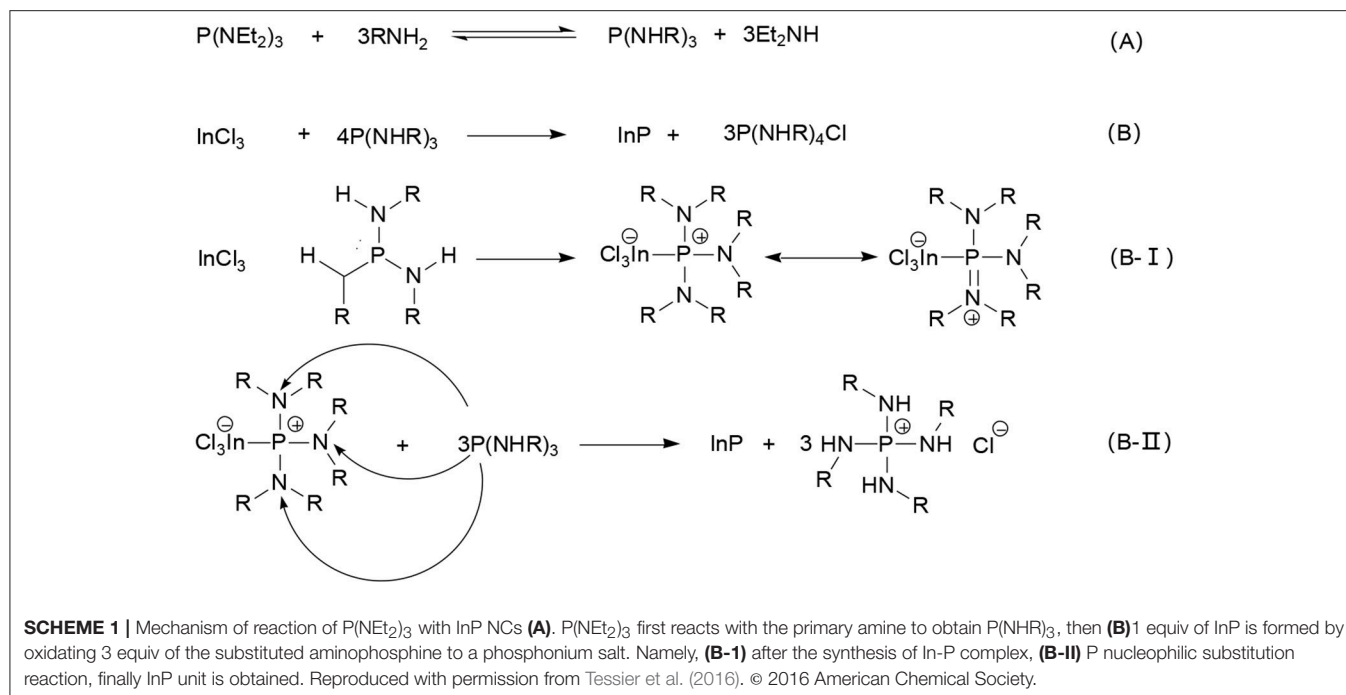
Since then, InP NCs with aminophosphine precursors have been further investigated: utilizing the precursors, the resulting green NCs achieved comparable PL performance to previous work with P(SiMe<sub>3</sub>)<sub>3</sub> (PLQY: 82 vs. 85%) (Jang et al., 2018). Tetrahedrally shaped InP NCs with improved stability ascribed to oleylamine and chloride ligands (Kim et al., 2016). Zinc salts were also found to activate the aminophosphine precursors by accelerating the formation of the In–P(I) pseudomonomer. Moreover, admixing Cd into a ZnSe shell could also be valid in synthesizing strain-free NCs, suppressing self-absorption, and reducing the amount of NCs for application (Dupont et al., 2017; Rafipoor et al., 2018). Cossairt et al. also demonstrated that aminophosphines were versatile precursors for metal phosphide NCs beyond InP (Mundy et al., 2018).

In short, InP NCs synthesized with aminophosphine precursor, have competitive properties to those from P(SiMe<sub>3</sub>)<sub>3</sub>

routes, indicating that aminophosphine is a promising option for the synthesis of InP NCs. Recently, mechanism of reaction and surface states has been confirmed by X-ray absorption spectroscopy, Raman scattering measurements, and NMR Spectroscopy, etc. (Janke et al., 2018; Laufersky et al., 2018; Tessier et al., 2018). These progresses indicate that synthesis of high quality and efficient InP NCs with the low cost, high stability, decent reactivity, and easy handling precursor will enable to obtain InP NCs on a large scale for a variety of applications, and lead to the extension of colloidal synthesis toward other pnictide NCs.

## INDIUM PHOSPHIDE NANOCRYSTALS

InP quantum emitting materials have been considered as an alternative substitution to the conventional quantum dots (QDs), with advantages of less toxicity. Technically speaking, the heavy metal of Cd or Pb in quantum dots-based electronics devices will cause minor environment issue because of the very low concentrations. These heavy metal issues can be further reduced to an even low level by appropriate encapsulation technique and recycling policy after disposal. However, the introduction of heavy-metal materials in electrical and electronic equipment has been restricted the regulation released by Restriction of Hazardous Substances Directive in the EU. Therefore, many researchers have shifted the interests from Cd or Pb based NCs to Cd-free alternatives, i.e., InP QDs.



Indeed, toxicological evaluation reveals that InP QDs display minor toxicity and decent bio-compatibility, thereby suggesting that they can be utilized for potential bio-imaging applications. For instance, Lin et al. found that no observable toxicity *in vivo* after intravenous injection of InP/ZnS QDs in mice for 84 days (Lin et al., 2015). Brunetti et al. studied the toxicity of CdSe/ZnS and InP/ZnS QDs *in vitro* as well as for *in vivo* applications (Brunetti et al., 2013). CdSe/ZnS QDs were shown to induce cell membrane damage, interference with  $\text{Ca}^{2+}$  homeostasis, which ascribed to the presence of  $\text{Cd}^{2+}$ , while InP/ZnS QDs exhibited low toxicity. Chibli et al. showed that the cytotoxicity induced by the generation of reactive oxygen species was shown to be significantly lower in the case of InP/ZnS QDs as compared to CdTe/ZnS QDs (Chibli et al., 2011). Taken together, toxicity studies demonstrate that these InP based QDs constitute a less toxic alternative to Cd based QDs. All these toxicity evaluations support that the InP QDs pose less environment concerns and guarantee the commercialization of InP QDs based electronics devices.

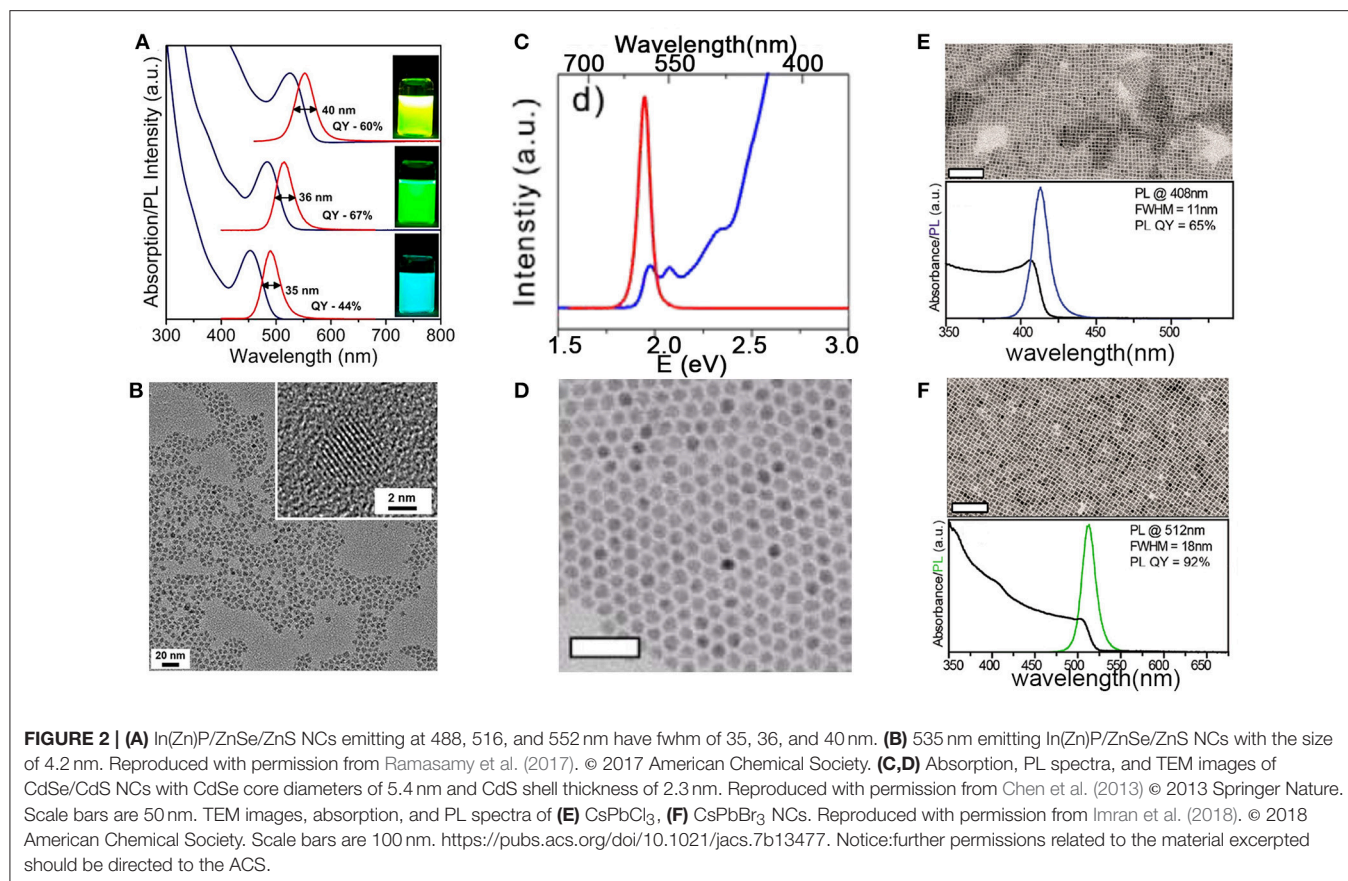
At the early stages, InP NCs were characterized as low PLQY, poor photo-stability, in particular its wide PL linewidth, in contrast to Cd-based NCs. In the following decades, the synthesis of InP NCs has achieved progress toward the improvements on the PLQY, PL stability, and narrowing the PL linewidth. **Figure 2** shows optical absorption, PL spectra, and TEM images of different NCs. The highest QY in literature for InP QDs was reported above 80%, which is close to unity PLQY of CdSe QDs and cesium lead halide perovskites ( $\text{CsPbX}_3$ ) NCs (Zhang et al., 2013; Nedelcu et al., 2015). Coating InP NCs with a shell can afford improved photostability, which allows for many applications. However, the wide PL linewidth limits their applications where narrow emission is required, i.e., multiple-color displays. The narrowest PL linewidth, estimated

as full-width at half maximum (fwhm), for InP-based core/shell or alloy NCs is 35 nm at 488 nm (**Figure 2A**) (Ramasamy et al., 2017), which is still inferior to CdSe QDs and  $\text{CsPbX}_3$  QDs.

In fact, intrinsic emission line width of InP NCs is comparable to CdSe NCs (**Figure 3A-IV**) (Cui et al., 2013), suggesting that the emission of InP NCs is heterogeneously broadened due to size distribution. The very broad size distribution of InP NCs indicates that separating nucleation and growth is difficult to achieve (Tamang et al., 2016), due to the more covalent nature of the III-V precursors and the fast depletion of precursors at high temperature (Allen et al., 2010).

Several methods have been used to improve size tunability and size distribution, including employing zinc chloride as reaction additive, and replacing  $\text{P}(\text{SiMe}_3)_3$  with lower cost, toxicity, and higher stability phosphorus precursors. Effects of Zn species in InP NC synthesis include the reduction of surface defects, facilitation of subsequent shell growth, and improvement of size distribution (Yang et al., 2012). The use of aminophosphine precursors ( $\text{P}(\text{NMe}_2)_3$  and  $\text{P}(\text{NEt}_2)_3$ ) enable the preparation of InP NCs with state-of-the-art quality in the literature.

Increasing core growth time also results in broadened size distribution of InP NCs. Hens et al. expanded this approach by replacing  $\text{P}(\text{NMe}_2)_3$  with  $\text{P}(\text{NEt}_2)_3$ , attaining a close to full yield conversion of indium precursor, and demonstrating size tuning was possible by changing the indium halide salt (Tessier et al., 2015). Changing of the precursor concentration is a size-tuning strategy, i.e., higher concentrations lead to smaller NCs, whereas decreasing the concentration appears to deteriorate the size distribution. Inspired by changing the free ligand concentration or the ligand chain length with CdSe NCs (Abe et al., 2013). Tessier and coworkers changed the indium salt halide. When all other reaction conditions were kept constant,



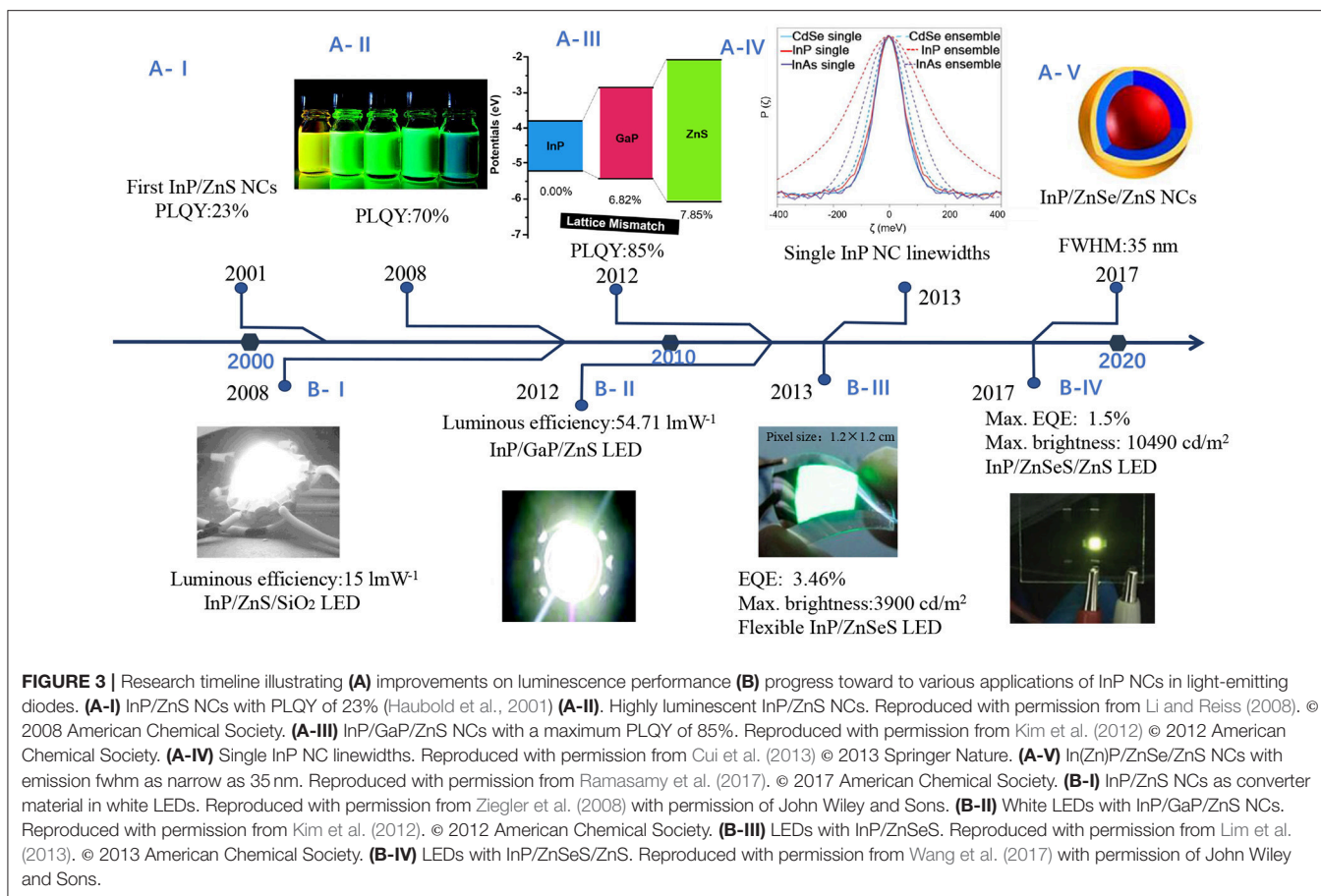
the first exciton position can be tuned from 570 to 550 or 520 nm by replacing InCl<sub>3</sub> by InBr<sub>3</sub> or InI<sub>3</sub>, respectively, allowing for an efficient size tuning by changing of the indium halide precursor.

Up to now, the narrowest emission of ensemble InP NCs were reported to be ca. 40 nm (Ramasamy et al., 2018), which is still wider than the line widths of PL acquired at the single particle level, suggesting that colloidal synthesis gave rise to the intrinsic inhomogeneity in InP NCs, that was previously attributed to broadened size distribution. Interestingly, recent report reveals that the broad emission may be caused by surface states and lattice disorder, that was confirmed by utilizing X-ray absorption spectroscopy and Raman scattering measurements (Janke et al., 2018). These findings suggest that developing new colloidal synthesis with the purpose of decreasing surface and lattice defects will be the future challenges to achieve comparable performance to CdSe NCs. Furthermore, dopant ions within lattice of NCs were found to be as important as control of the surface states to obtain bright dopant emission (Pu et al., 2017). Ag<sup>+</sup> dopants can be introduced into lattice of CdSe NCs precisely (Sahu et al., 2012), while few works exist on the doped InP NCs. Recent reports demonstrate that Ag and Cu are of interest as doping agents for dual-emissive InP NCs, therefore, the NCs have potential applications in biological and LEDs applications (Zhang et al., 2015; Yang et al., 2017; Vinokurov et al., 2018). In conclusion, synthetic development specifically for these applications is an interesting avenue to explore.

So far, quite limited progress has been achieved in shape control of InP NCs, only tetrahedral (Kim et al., 2016) and spherical NCs are reported. Colloidal nanoplatelets differ from NCs due to the strong quantum confinement acting in one dimension, which have been most extensively studied. CdSe nanoplatelets can be synthesized with a thickness controlled with monolayer precision, gaining access to a wide spectral range (Christodoulou et al., 2018). Hence, as for InP, development of such 2D heterostructures can be a promising and exciting future direction.

## INDIUM PHOSPHIDE-BASED CORE/SHELL NANOCRYSTALS

The concept of core/shell in NCs has been widely implemented for the conventional CdSe based core/shell structures. Coating an additional shell around the initial seeds provides extra means to manipulate their properties. The obvious benefit is allowing one to easily obtain NCs with enhanced fluorescence efficiency and improved stability against photo-oxidation. This is of particularly importance for the InP NCs, because even freshly synthesized colloidal InP NCs exhibit PLQY of <1% due to surface defects related to P atoms. Talapin et al. found that treating InP NCs with HF can reconstruct the surface and enhance the PLQY up to 40% (Adam et al., 2005). Besides, InP NCs without protecting shell are prone to surface oxidation and photodegradation. Therefore,



coating InP with a passivating shell is the prerequisite for further their applications.

Most importantly, band gap offsets and lattice strain between core and shell significantly modify the intraband and interband states, and affect the carrier dynamics of exciton (Dupont et al., 2017; Rafipoor et al., 2018). Therefore, it is possible to prepare the core/shell QDs with unusual and practical photophysical properties. Brainis found that a thick ZnSe shell coating is helpful to reach nearly non-blinking NCs (Chandrasekaran et al., 2017). Hollingsworth et al. reported that coating InP NCs with 11 monolayers of CdS can significantly increase the bi-exciton lifetime up to 7 ns, indicating dramatic suppression of nonradiative Auger recombination (Dennis et al., 2012). So far, ZnSe and ZnS are often used as shell materials for the obvious reason of their large band gap and low toxicity. Herein, we will summarize recent progress toward the synthesis of InP based core/shell direction.

The first issue encountered in the synthesis of core/shell structured InP/ZnSe and InP/ZnS NCs is the relatively large lattices mismatch. In case of former is 3.3%, and in the latter is approaching to 7.7%. The epitaxial growth of shell on top of InP NCs has been proved to be challenging, due to the large lattice constant ( $a = 5.93 \text{ \AA}$ ). Besides, defects may exist due to the strain at the core/shell interfaces induced by lattice mismatch. Therefore, finding appropriate strategies to avoid

defect formation represents one of the main challenges in the synthesis of InP based core/shell NCs.

Overcoating the NCs with a shell of ZnS leads to high PLQY, as shown in Figure 3A. Haubold et al. first passivated the InP core with ZnS, enhanced the PLQY to 23% (Figure 3A-I) (Haubold et al., 2001). They used diethylzinc and bis(trimethylsilyl) sulfide to grow ZnS on InP NCs at  $260^\circ\text{C}$  for a limited time, aiming to avoid Ostwald ripening. TEM images and XPS data indicated the formation of ZnS passivated InP NCs. Then one-pot synthesis without precursor injection gave access to InP/ZnS NCs with a maximum PLQY of 70% (Figure 3A-II), narrow emission line width (40–60 nm fwhm) and excellent photostability (Li and Reiss, 2008). The high PLQY is likely attributed to the “smooth” core/shell interface with few defect states. So far, the highest PLQY (85%) (Figure 3A-III) has been reported for the InP/GaP/ZnS NCs with superior photostability as compared to InP/ZnS NCs (Kim et al., 2012), where  $\text{In}^{3+}$  ions are effectively replaced by  $\text{Ga}^{3+}$  ions near the surface. The intermediate layer GaP mitigates the effect of lattice mismatch between InP and ZnS. Lattice strain with a ZnS shell may limit a shell thickness  $< 1 \text{ nm}$ , making NCs vulnerable against degradable conditions. To alleviate lattice strain, Lee et al. used ZnSe as a lattice adaptor to achieve thicker shells (1.9 nm), the NCs exhibited high PLQY, and enhanced stability under UV irradiation, ligand exchange or rigorous purification (Lim et al., 2011).

Pietra et al. found that  $\text{In}_x\text{Zn}_y\text{P}$  alloy NCs with a tunable lattice constant can be prepared by changing the amount of zinc precursor, which can match a chosen shell material, possibly creating strain-free core/shell NCs (Pietra et al., 2016). As a result, PLQY of  $\text{InZnP/ZnSeS}$  NCs can reach as high as 60%. Optical spectra, PLQY and TEM images of  $\text{In}_x\text{Zn}_y\text{P}$  NCs are shown in **Figures 4A–C**. They also found that a preferential Ga-for-Zn cation exchange led to a  $\text{InZnP/InGaP}$  core/shell system with increased PLQY when  $\text{Zn/In} \geq 0.5$ . Another GaP and ZnSeS outer shell of  $\text{InZnP/InGaP}$  NCs exhibit enhanced PLQY (over 70%) and stability (Pietra et al., 2017). Structure and optical spectra of  $\text{InZnP/InGaP/GaP/ZnSeS}$  NCs are shown in **Figures 4D–F**.

## COLLOIDAL SYNTHESIS OF II–V METAL PHOSPHIDE NANOCRYSTALS

Cadmium phosphide has been the subject of intensive interest owing to its unique physical properties.  $\text{Cd}_2\text{P}_3$  is a narrow bandgap semiconductor (0.55 eV in bulk) with high dielectric constant (5.8), large Bohr exciton radius (36 nm). All these features suggest that  $\text{Cd}_2\text{P}_3$  in quantum-dot form presents a new material with emission wavelengths span the visible through the near-infrared.

Miao et al. for the first time, reported the colloidal synthesis of cadmium phosphide NCs using  $\text{P}(\text{SiMe}_3)_3$  as a phosphorus precursor in the presence of oleylamine and trioctylphosphine as ligands (Miao et al., 2010). By varying the temperature and growth time, they obtained high quality  $\text{Cd}_3\text{P}_2$  NCs with tunable emission ranging from 650 to 1,200 nm, and with high PLQY up to ca. 40%. Further research from the same group found that replacing  $\text{P}(\text{SiMe}_3)_3$  by  $\text{PH}_3$  will reach cadmium phosphide NCs with different stoichiometric ( $\text{Cd}_6\text{P}_7$  instead of  $\text{Cd}_3\text{P}_2$ ), and improved size distribution (Miao et al., 2012). **Figure 5A** shows the absorption spectra with multiple transition of  $\text{Cd}_6\text{P}_7$  NCs for the first time. TEM images in **Figure 5B** show that  $\text{Cd}_6\text{P}_7$  NCs are monodisperse with nearly spherical shape, and the average size of NCs is  $6.5 \pm 0.3$  nm. Since  $\text{PH}_3$  is less reactive compared to  $\text{P}(\text{SiMe}_3)_3$ , size of NCs is well controlled by the low reaction rate. This simple and inexpensive strategy paves the way to large-scale production of metal phosphide NCs.

Xie et al. reported an advanced synthesis of  $\text{Cd}_3\text{P}_2$  NCs using  $\text{P}(\text{SiMe}_3)_3$  as a phosphorus precursor and using oleic acid as the only ligand (Xie et al., 2010). They found that under these conditions, the size of the obtained NCs can be tuned in in the range of 1.6–12 nm by simply adjusting the concentration of the oleic acid. **Figure 5C** shows PL spectra of  $\text{Cd}_3\text{P}_2$  NCs with various sizes, which covers the whole visible and near-IR (450 to over 1,500 nm) region. The optical properties make the NCs useful in optical amplification and lighting. TEM images of  $\text{Cd}_3\text{P}_2$  NCs with 12 nm are given in **Figure 5D**, where a square array of the NCs is observed.

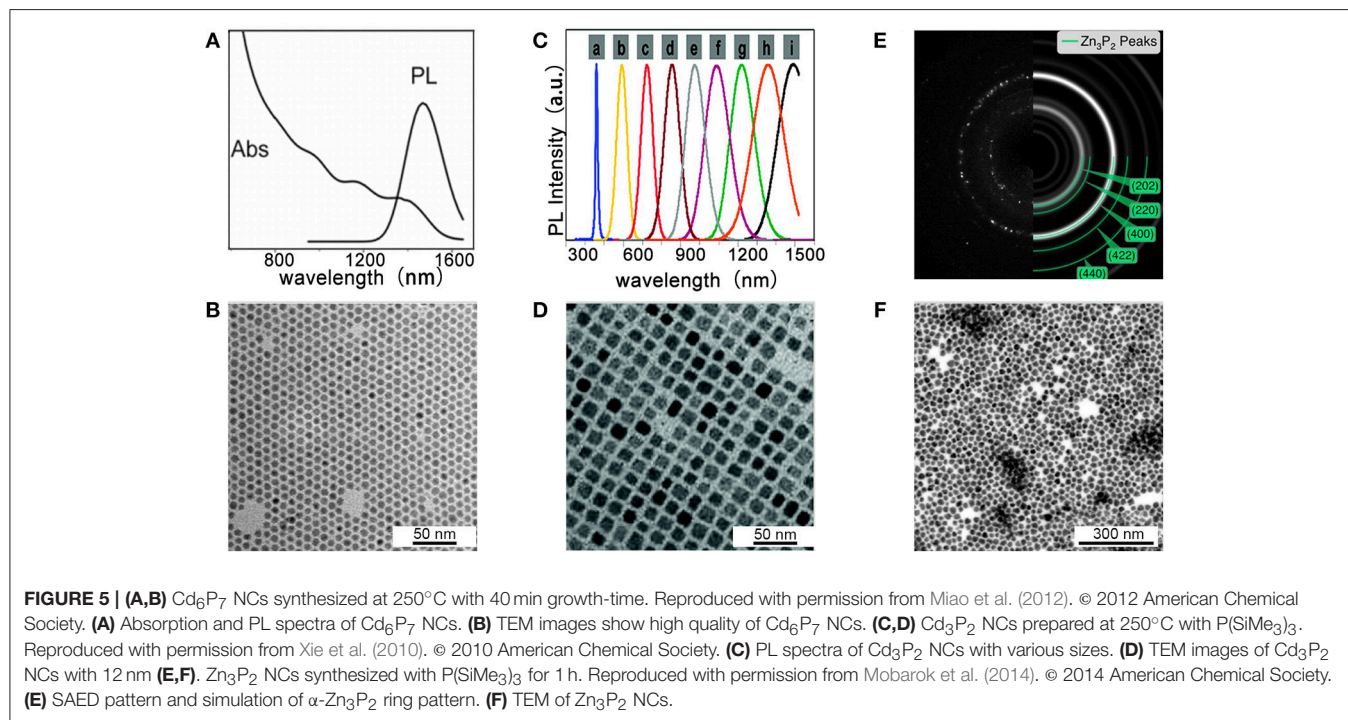
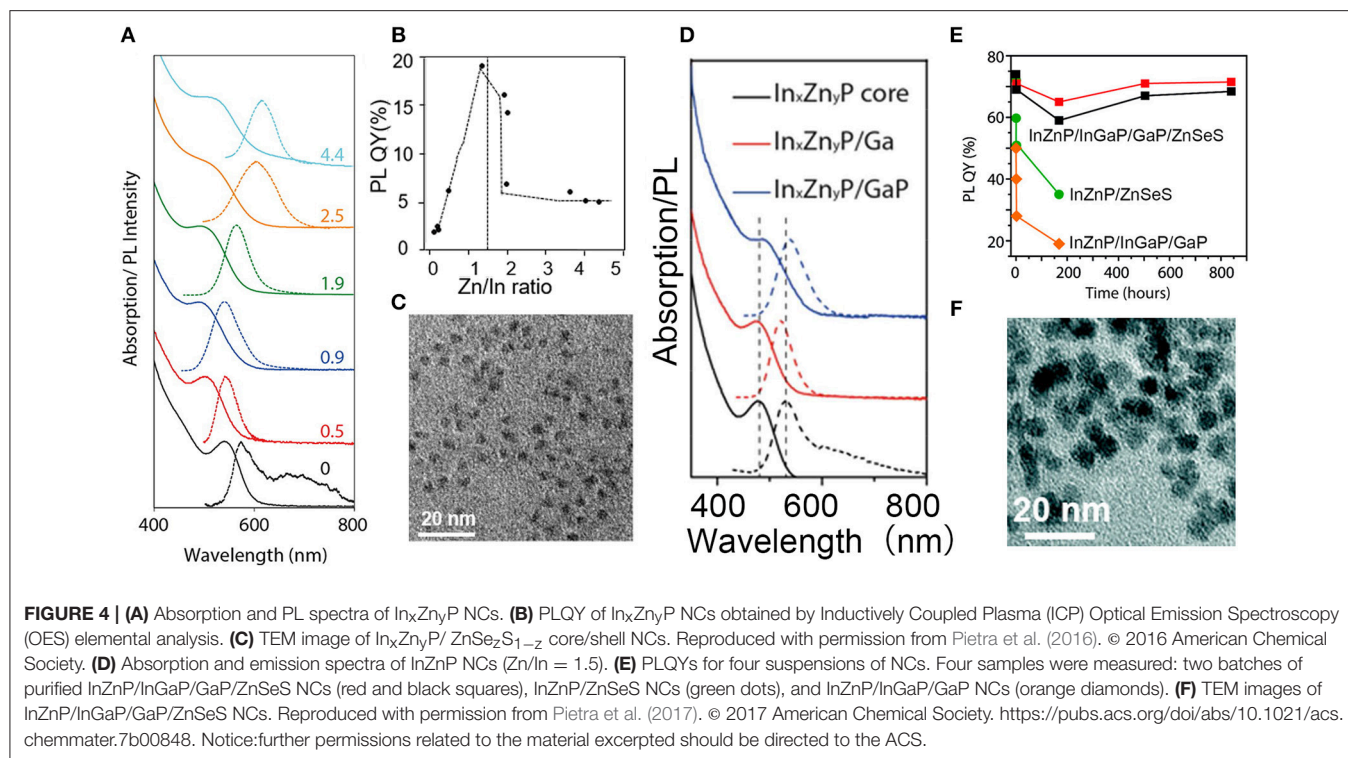
Cadmium phosphide NCs in the absence of protecting shell can be easily oxidized, which hinders their application in open air. Delpech reported a method for the coating of cadmium

phosphide NCs (Ojo et al., 2012). The coating procedure was performed by using zinc acetate and ethylene sulfide as the zinc and sulfur precursors, respectively. They obtained high-quality  $\text{Cd}_3\text{P}_2/\text{ZnS}$  NCs with PLQY over 50% with modest air stability.

Zinc phosphide ( $\text{Zn}_3\text{P}_2$ ) has great potential as a solar absorber in thin film photovoltaics, because of its high absorption coefficient in the order of  $10^{-4}$ – $10^{-5} \text{ cm}^{-1}$ , large carrier diffusion length of 5–10  $\mu\text{m}$ , mostly importantly suitable band gap of 1.5 eV (Green and O'Brien, 2001). The band gap of  $\text{Zn}_3\text{P}_2$  is very close that of CdTe and slightly narrower than CdSe, indicating its high solar absorption capability. Fabrication of  $\text{Zn}_3\text{P}_2$  in the quantum size has been intensively pursued for a long time, because  $\text{Zn}_3\text{P}_2$  NCs can potentially be an emitting material like CdTe and CdSe NCs (Luber et al., 2013). Besides,  $\text{Zn}_3\text{P}_2$  exhibits superior features in contrast to CdTe, CdSe, and InP, because both the Zn and the P are nontoxic and earth abundant elements.

Up to now, there have been several reports on the synthesis of  $\text{Zn}_3\text{P}_2$  NCs. The reported synthetic approaches of colloidal  $\text{Zn}_3\text{P}_2$  NCs borrow experiences from the synthesis of other metal phosphide NCs, utilizing the same phosphorus precursor, such as  $\text{P}_4$ , TOP,  $\text{PH}_3$ , and  $\text{P}(\text{SiMe}_3)_3$  and the same ligands such as TOP. The zinc precursor includes dimethylzinc, diethylzinc, and zinc stearate. It is worth noting that the formation of  $\text{Zn}_3\text{P}_2$  compounds in liquid solution is difficult compared with other metal phosphides. For instance, significant quantity of  $\text{ZnCl}_2$  is often used, during the synthesis of InP NCs. However, Extensive analysis suggests that under the conditions of the InP synthesis, zincs are not incorporated into the core of the final InP NCs. This feature explains the reason that early reports on the synthesis of NCs usually give poor crystalline and low PL product. This is also consistent with many observations that the synthesis of  $\text{Zn}_3\text{P}_2$  NCs requires much higher temperatures.

Green reported the first colloidal synthesis of  $\text{Zn}_3\text{P}_2$  NCs displaying quantum confined emission (Green and O'Brien, 2001). The synthesis was performed by using dimethylzinc as zinc precursor and the primary phosphine  $\text{H}_2\text{P}^t\text{Bu}$  as phosphorus source. The obtained particles were revealed as a mixture of both crystalline and amorphous materials. Miao et al. reported the synthesis of  $\text{Zn}_3\text{P}_2$  NCs by using either gas  $\text{PH}_3$  or  $\text{P}(\text{SiMe}_3)_3$  as phosphorus precursor and diethylzinc or zinc stearate as the zinc source (Miao et al., 2013) Buriak and coworkers synthesized monodisperse and pure crystalline  $\text{Zn}_3\text{P}_2$  NCs at low temperature (Mobarok et al., 2014). From the selected area electron diffraction (SAED) pattern in **Figure 5E** and XRD spectrum, these NCs were found to possess the crystalline tetragonal  $\alpha$ - $\text{Zn}_3\text{P}_2$  structure. TEM image in **Figure 5F** shows the average size of NCs is  $14.7 \pm 2.1$  nm, with a distribution of 14%. In general, to date the reported synthesis of  $\text{Zn}_3\text{P}_2$  NCs is more limited than cadmium and indium based NCs, mostly likely due to the large differences in reactivity between traditional zinc and cadmium precursors with conventional pnictide sources. Literature on colloidal  $\text{Zn}_3\text{P}_2$  NCs mainly focuses on designing the synthesis and understanding the structure and properties of the NCs instead of their practical device application.



## COLLOIDAL SYNTHESIS OF TRANSITION METAL PHOSPHIDE NANOCRYSTALS

Recently, transition metal phosphide NCs have attracted intense interest for their potential in catalysis, magnetic recording

media, and as anode materials in lithium ion batteries (Bichat et al., 2004b; Brock and Senevirathne, 2008). Among these, iron phosphides exist in a wide range of stoichiometry, their properties depend on their physical and electronic structures, such as  $\text{Fe}_3\text{P}$  and  $\text{Fe}_2\text{P}$  are ferromagnetic,  $\text{FeP}$  is super magnetic,

$\text{FeP}_2$  and  $\text{FeP}_4$  are antimagnetic semiconductors (Blanchard et al., 2008).  $\text{Cu}_3\text{P}$  NCs are air-stable and environmentally friendly materials. When they are used in batteries, their theoretical weight capacitances are slightly higher than that of graphite, and volumetric capacities are more than three times greater than that of graphite (Bichat et al., 2004a).

Nowadays, TOP is often used as a phosphorus precursor in the synthesis of transition metal phosphide NCs. Schaak et al. reported the colloidal synthesis of  $\text{Cu}_3\text{P}$  NCs for the first time, by injecting the Cu NCs and TOP into the TOPO at high temperature (Henkes and Schaak, 2007). It is found that metals can cause cleavage of the P-C bond, resulting in diffusion of phosphorus into the metal. Falqui et al. optimized the synthesis by replacing Cu NCs with cuprous chloride ( $\text{CuCl}$ ) to react with TOP, and obtained  $\text{Cu}_3\text{P}$  NCs with improved size distributions (De Trizio et al., 2012). The ratio of TOP and  $\text{CuCl}$  determined  $\text{Cu}_3\text{P}$  NCs either by a direct formation of  $\text{Cu}_3\text{P}$  nucleation or by forming Cu NCs first and then converting into  $\text{Cu}_3\text{P}$  NCs. The former way leads to reproducible and size controllable pure  $\text{Cu}_3\text{P}$ , while the latter way results in the formation of Cu- $\text{Cu}_3\text{P}$  Janus-like NCs, which is unsuitable for applications in batteries with larger copper domains. Manna et al. reported the synthesis of by using  $\text{PH}_3$  as the P precursor (Manna et al., 2013). The synthesis can be performed under relatively lower reaction temperature. The obtained  $\text{Cu}_3\text{P}$  nanoplatelets was found to be single crystalline and possess the semiconducting, plasmonic, and rectification properties. More recently, Liu et al. used the more active  $\text{P}(\text{SiMe}_3)_3$  as the P precursor and prepared the  $\text{Cu}_{3-x}\text{P}$  NCs at very low reaction temperature (Liu et al., 2016). They further demonstrated that the localized surface plasmon resonance and nonlinear optical absorption of the  $\text{Cu}_{3-x}\text{P}$  NCs can be modulated by thermal treatment.

Perera et al. firstly reported the synthesis of iron phosphides NCs by reaction of  $\text{Fe}(\text{acac})_3$  with  $\text{P}(\text{SiMe}_3)_3$  in TOPO at  $260^\circ\text{C}$ , resulting product in pure FeP phase, round shape, narrow size distribution, and high colloidal stability (Perera et al., 2003; Brock and Senevirathne, 2008). Park and coworkers synthesized uniform-sized FeP and  $\text{Fe}_2\text{P}$  nanorods from thermal decomposition of iron-phosphine complexes (Park et al., 2005). Schaak et al. reported the synthesis of FeP NCs by using pre-synthesized Fe NCs to react with TOP in hexadecylamine (Henkes and Schaak, 2007). Recently, Liu et al. used inexpensive and air-stable triphenyl phosphite (**Figure 6A**) as the phosphorus sources and prepared rod-shaped  $\text{Fe}_2\text{P}$  NCs (Liu et al., 2018). **Figure 6** displays representative TEM images of the  $5 \pm 1 \text{ nm} \times 22 \pm 5 \text{ nm}$  rod-shaped  $\text{Fe}_2\text{P}$  nanoparticles (**Figures 6B,C**),  $4.5 \pm 1 \text{ nm} \times 17 \pm 1 \text{ nm}$  disk-shaped  $\text{Cu}_3\text{P}$  nanoparticles (**Figures 6E,F**).

## APPLICATION

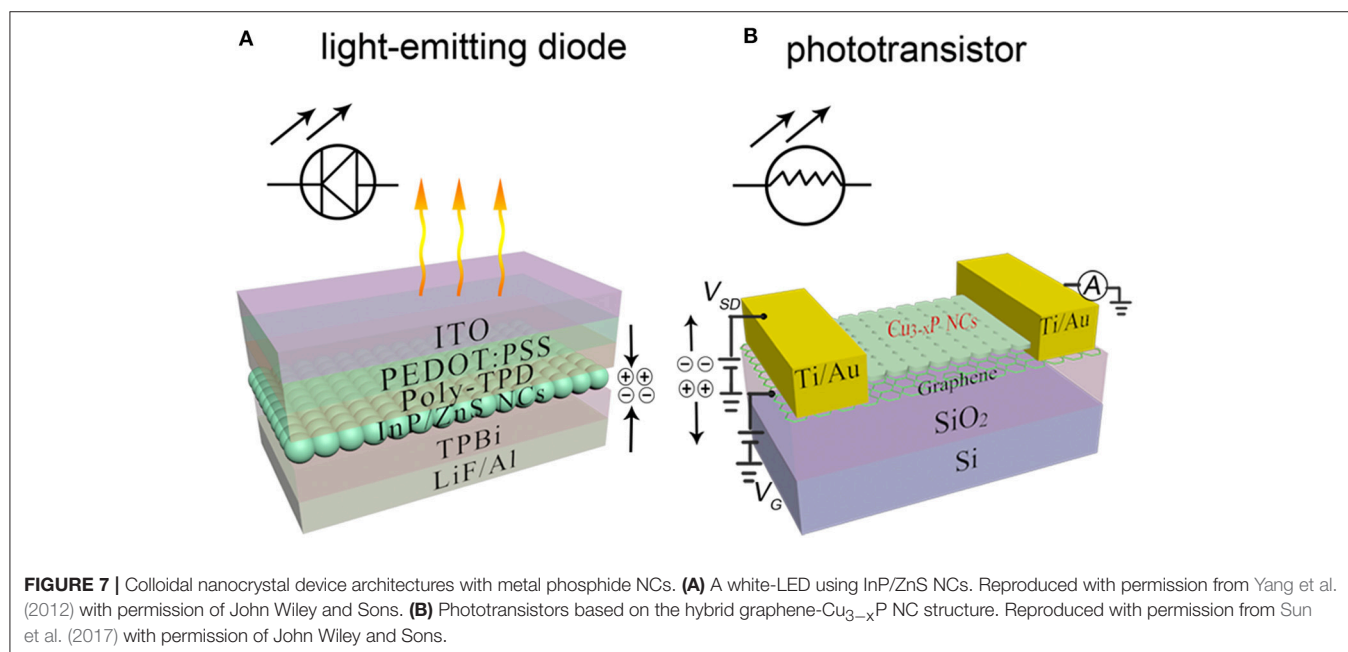
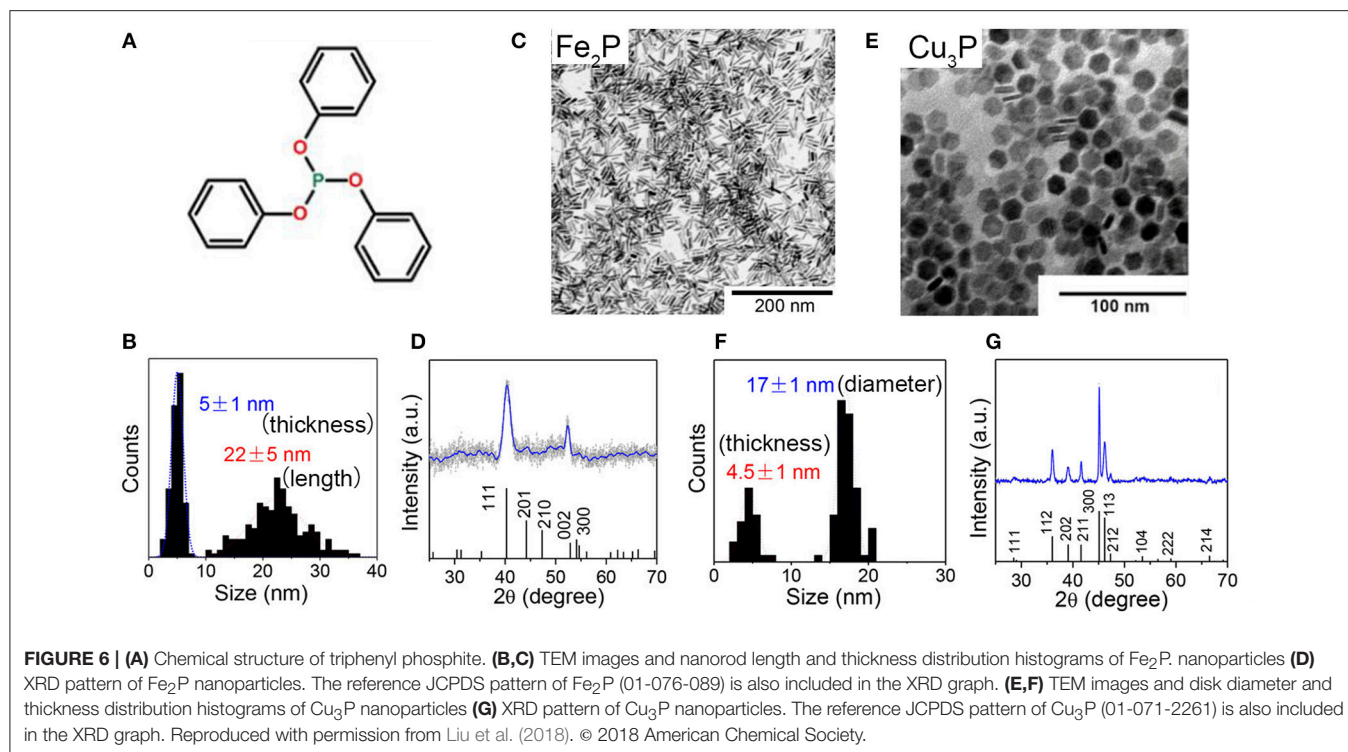
Colloidal NCs are covered by a layer of ligands, which can stabilize the colloidal NCs in suitable solvents. This unique feature enables the fabrication of thin film electronic devices by well-established coating and printing techniques. In view of great progress toward the synthesis by means of inexpensive

and scalable, wet-chemical synthetic procedures, colloidal QDs are emerging as a versatile class material in electronic devices, in contrast to expensive physically manufacturing processes. Besides, colloidal NCs open up new opportunities to integrate inorganic semiconductor devices with advanced features such as high-performance, large-area, and flexibility.

Among them, colloidal metal phosphide NCs offer a powerful platform for solution-processable electronic and optoelectronic devices, including photodetectors (Keuleyan et al., 2011), photovoltaic cells and light-emission devices (Steckel et al., 2003; Li et al., 2008; Qian et al., 2011), as shown in **Figure 7**. The actual active element in electronic and optoelectronic devices is macroscopic array of NCs (Talpin et al., 2010), which act as the key components with functions of light absorption or emission and charge transportation (Gaponenko et al., 2016; Kagan et al., 2016). **Figure 3B** shows progress toward to various applications of InP NCs in LEDs.

Commercialization of conventional quantum dots-based lighting emitting diodes are facing the strict regulation on the using of hazardous substances, such as Cd and Pb. Recent progress toward the synthesis of high-quality InP QDs provides a solution to address this issue. InP QDs have been widely applied in white lighting emitting devices as down conversion phosphor (Ziegler et al., 2008; Yang et al., 2012) and in the framework of electroluminescence devices (Lim et al., 2013; Shen et al., 2017; Wang et al., 2017; Ramasamy et al., 2018). Lim et al. reported design of InP QDs based electroluminescence light emitting diodes (Lim et al., 2013). The device structure based on InP QDs is shown in **Figure 7A**. By optimizing the charge balance, they observed direct formation of exciton within QDs and efficient radiative exciton recombination. The external quantum efficiency is reported as 3.46% and brightness is  $3,900 \text{ cd m}^{-2}$ . In a recent report, the brightness was improved to  $10,000 \text{ cd m}^{-2}$  by using ZnMgO as the electron transporting layer to improve the electron injection (Wang et al., 2017). The effect of Auger recombination, Förster resonant energy transfer among the closely packed QDs in a thin film of QLEDs, have a negative effect on device efficiency of QLED. Thus, thick shells or interfacial alloy layer acting as an effective spacer can suppress the above effects. A record of external quantum efficiency of 6.6% in heavy-metal-free red QLEDs have been achieved with a thick ZnS shell of InP/ZnSe/ZnS QDs (15 nm) (Cao et al., 2018). That means there is still more room for improvement and optimization. Moreover, replacing red, green, blue (RGB) color filters with narrow-band green, red InP/ZnSeS/ZnS QD films in color-by-blue QD-emissive liquid-crystal displays (LCDs) results in 1.49 times greater in the relative luminance levels, 2.42 times higher in EQE values than conventional color filter (CF)-LCD, making it possible to replace conventional RGB CF-assisted LCDs (Kang et al., 2018).

$\text{Cd}_3\text{P}_2$  NCs and  $\text{Zn}_3\text{P}_2$  NCs have been considered as promising materials for photovoltaic applications. Cao et al. proposed  $\text{PbS}/\text{Cd}_3\text{P}_2$  quantum heterojunction for NC photovoltaic cells, where p- and n-layers were quantum-tunable and solution-processed infrared light absorbers (Cao et al., 2015). The increased thickness of an n-layer type  $\text{Cd}_3\text{P}_2$  from



one layer to two layers resulted in devices exhibiting a power conversion of 1.5%, with an open-circuit voltage of 0.39 V, a short-circuit current of 8.4 mA cm<sup>-2</sup> and a fill factor of 45%. Luber and coworkers tested photovoltaic performance of heterojunction devices consisting of ITO/ZnO/Zn<sub>3</sub>P<sub>2</sub>/MoO<sub>3</sub>/Ag (Luber et al., 2013). The device possessed excellent rectification behavior (rectification ratio of 600) and photosensitivity (on/off

ratio of ~10<sup>2</sup> under 100 mW cm<sup>-2</sup> AM 1.5G illumination). Charge carrier mobilities and lifetimes for InP and InZnP QDs are comparable to those of PbS QDs after an (NH<sub>4</sub>)<sub>2</sub>S ligand-exchange procedure, making it possible to utilize In(Zn)P QD films in solar cells. Power conversion efficiencies of 0.65 and 1.2% were achieved of the solar cells based on InP and InZnP QDs, respectively (Crisp et al., 2018).

Recently, Sun demonstrated high-performance, broadband photodetectors with the hybrid graphene-Cu<sub>3-x</sub>P NC structure (Sun et al., 2017). The efficient three-terminal photodetectors (phototransistors) (**Figure 7B**) exhibit photoresponse from 400 to 1,550 nm with an ultrahigh responsivity ( $1.59 \times 10^5 \text{ A W}^{-1}$ ) and high photoconductive gain ( $6.66 \times 10^5$ ) at 405 nm, and a good responsivity of  $9.34 \text{ A W}^{-1}$  at 1,550 nm. The light-activated functionality of device is provided by a layer of strongly light-absorbing colloidal NCs and an ultrafast carrier transportation graphene layer.

In summary, the prospect of employing metal phosphide NCs in optoelectronic devices offers a number of unique benefits related to their photo-physical properties. Therefore, the colloidal synthesis of various types of metal phosphide NCs has been steadily increasing in recent years and further stimulates their applications. Among them, InP, Cd<sub>3</sub>P<sub>3</sub>, and Zn<sub>3</sub>P<sub>2</sub> NCs are of significant importance in many light absorption and emission-based applications, such as photovoltaics and light emitting diodes. Particularly, InP and Zn<sub>3</sub>P<sub>3</sub> are of great interest due to their suitable band gap and low intrinsic toxicity. Despite excellent properties, they are still facing critical issues before they can replace conventional NCs. Compared to chalcogenide-based NCs, metal phosphide NCs exhibit

synthetically induced broad size distributions, and low PLQYs and poor thermo- and photo-stability stability. Significant attention has been given to improving these aspects, from viewpoint of chemistry. However, additional attention must be paid to the optimization of their photo-physical properties via structure engineering at the interface and controlling the exciton dynamics. Currently, the performance of optoelectronic devices based on metal phosphide NCs is largely limited due to the undeveloped synthetic methods. Future development of the synthetic approach for metal phosphide NCs is expected to lead to the high-performance optoelectronic devices, i.e., displays.

## AUTHOR CONTRIBUTIONS

All authors listed have made a substantial, direct and intellectual contribution to the work, and approved it for publication.

## ACKNOWLEDGMENTS

We gratefully appreciate the financial support from the National Natural Science Foundation of China (21701015 and 21811530054).

## REFERENCES

- Abe, S., Capek, R. K., De Geyter, B., and Hens, Z. (2013). Reaction chemistry/nanocrystal property relations in the hot injection synthesis, the role of the solute solubility. *ACS Nano* 7, 943–949. doi: 10.1021/nn3059168
- Adam, S., Talapin, D. V., Borchert, H., Lobo, A., McGinley, C., de Castro, A. R. B., et al. (2005). The effect of nanocrystal surface structure on the luminescence properties: photoemission study of HF-etched InP nanocrystals. *J. Chem. Phys.* 123:084706. doi: 10.1063/1.2004901
- Allen, P. M., Walker, B. J., and Bawendi, M. G. (2010). Mechanistic insights into the formation of InP quantum dots. *Angew. Chem. Int. Edn.* 49, 760–762. doi: 10.1002/anie.200905632
- Bang, E., Choi, Y., Cho, J., Suh, Y. H., Ban, H. W., Son, J. S., et al. (2017). Large-scale synthesis of highly luminescent InP@ZnS quantum dots using elemental phosphorus precursor. *Chem. Mater.* 29, 4236–4243. doi: 10.1021/acs.chemmater.7b00254
- Bichat, M. P., Politova, T., Pascal, J. L., Favier, F., and Monconduit, L. (2004a). Electrochemical reactivity of Cu<sub>3</sub>P with lithium. *J. Electrochem. Soc.* 151, A2074–A2081. doi: 10.1149/1.1815156
- Bichat, M. P., Politova, T., Pfeiffer, H., Tancret, F., Monconduit, L., Pascal, J. L., et al. (2004b). Cu<sub>3</sub>P as anode material for lithium ion battery: powder morphology and electrochemical performances. *J. Power Sources* 136, 80–87. doi: 10.1016/j.jpowsour.2004.05.024
- Blanchard, P. E. R., Grosvenor, A. P., Cavell, R. G., and Mar, A. (2008). X-ray photoelectron and absorption spectroscopy of metal-rich phosphides M<sub>2</sub>P and M<sub>3</sub>P (M = Cr–Ni). *Chem. Mater.* 20, 7081–7088. doi: 10.1021/cm802123a
- Brock, S. L., and Senevirathne, K. (2008). Recent developments in synthetic approaches to transition metal phosphide nanoparticles for magnetic and catalytic applications. *J. Solid State Chem.* 181, 1552–1559. doi: 10.1016/j.jssc.2008.03.012
- Brunetti, V., Chibli, H., Fiammengio, R., Galeone, A., Malvindi, M. A., Vecchio, G., et al. (2013). InP/ZnS as a safer alternative to CdSe/ZnS core/shell quantum dots: in vitro and in vivo toxicity assessment. *Nanoscale* 5, 307–317. doi: 10.1039/C2NR33024E
- Cao, F., Wang, S., Wang, F. J., Wu, Q. Q., Zhao, D. W., and Yang, X. Y. (2018). A layer-by-layer growth strategy for large-size InP/ZnSe/ZnS core-shell quantum dots enabling high-efficiency light-emitting diodes. *Chem. Mater.* 30, 8002–8007. doi: 10.1021/acs.chemmater.8b03671
- Cao, H. F., Liu, Z. K., Zhu, X. X., Peng, J., Hu, L., Xu, S. M., et al. (2015). PbS/Cd<sub>3</sub>P<sub>2</sub> quantum heterojunction colloidal quantum dot solar cells. *Nanotechnology* 26:035401. doi: 10.1088/0957-4484/26/3/035401
- Carenco, S., Demange, M., Shi, J., Boissiere, C., Sanchez, C., Le Floch, P., et al. (2010). White phosphorus and metal nanoparticles: a versatile route to metal phosphide nanoparticles. *Chem. Commun.* 46, 5578–5580. doi: 10.1039/c0cc00684j
- Carenco, S., Portehault, D., Boissiere, C., Mezailles, N., and Sanchez, C. (2013). Nanoscaled metal borides and phosphides: recent developments and perspectives. *Chem. Rev.* 113, 7981–8065. doi: 10.1021/cr400020d
- Chandrasekaran, V., Tessier, M. D., Dupont, D., Geiregat, P., Hens, Z., and Brainis, E. (2017). Nearly blinking-free, high-purity single-photon emission by colloidal InP/ZnS quantum dots. *Nano Lett.* 17, 6104–6109. doi: 10.1021/acs.nanolett.7b02634
- Chen, O., Zhao, J., Chauhan, V. P., Cui, J., Wong, C., Harris, D. K., et al. (2013). Compact high-quality CdSe–CdS core-shell nanocrystals with narrow emission linewidths and suppressed blinking. *Nat. Mater.* 12, 445–451. doi: 10.1038/nmat3539
- Chibli, H., Carlini, L., Park, S., Dimitrijevic, N. M., and Nadeau, J. L. (2011). Cytotoxicity of InP/ZnS quantum dots related to reactive oxygen species generation. *Nanoscale* 3, 2552–2559. doi: 10.1039/c1nr10131e
- Christodoulou, S., Climente, J. I., Planelles, J., Brescia, R., Prato, M., Martin-Garcia, B., et al. (2018). Chloride-Induced thickness control in CdSe nanoplatelets. *Nano Lett.* 18, 6248–6254. doi: 10.1021/acs.nanolett.8b02361
- Clark, M. D., Kumar, S. K., Owen, J. S., and Chan, E. M. (2011). Focusing nanocrystal size distributions via production control. *Nano Lett.* 11, 1976–1980. doi: 10.1021/nl200286j
- Coe, S., Woo, W. K., Bawendi, M., and Bulovic, V. (2002). Electroluminescence from single monolayers of nanocrystals in molecular organic devices. *Nature* 420, 800–803. doi: 10.1038/nature01217
- Crisp, R. W., Kirkwood, N., Grimaldi, G., Kinge, S., Siebbeles, L. D. A., and Houtepen, A. J. (2018). Highly photoconductive InP quantum dots films and solar cells. *ACS Appl. Energy Mater.* 1, 6569–76. doi: 10.1021/acsaem.8b01453

- Cui, J., Beyler, A. P., Marshall, L. F., Chen, O., Harris, D. K., Wanger, D. D., et al. (2013). Direct probe of spectral inhomogeneity reveals synthetic tunability of single-nanocrystal spectral linewidths. *Nat. Chem.* 5, 602–606. doi: 10.1038/nchem.1654
- Dai, X. L., Zhang, Z. X., Jin, Y. Z., Niu, Y., Cao, H. J., Liang, X. Y., et al. (2014). Solution-processed, high-performance light-emitting diodes based on quantum dots. *Nature* 515, 96–99. doi: 10.1038/nature13829
- De Trizio, L., Figuerola, A., Manna, L., Genovese, A., George, C., Brescia, R., et al. (2012). Size-tunable, hexagonal plate-like Cu<sub>3</sub>P and Janus-like Cu-Cu<sub>3</sub>P Nanocrystals. *ACS Nano* 6, 32–41. doi: 10.1021/nn203702r
- Dennis, A. M., Mangum, B. D., Piryatinski, A., Park, Y. S., Hannah, D. C., Casson, J. L., et al. (2012). Suppressed blinking and Auger recombination in near-infrared type-II InP/CdS nanocrystal quantum dots. *Nano Lett.* 12, 5545–5551. doi: 10.1021/nl302453x
- Dupont, D., Tessier, M. D., Smet, P. F., and Hens, Z. (2017). Indium phosphide-based quantum dots with shell-enhanced absorption for luminescent down-conversion. *Adv. Mater.* 29:1700686. doi: 10.1002/adma.201700686
- Friedfeld, M. R., Stein, J. L., and Cossairt, B. M. (2017). Main-group-semiconductor cluster molecules as synthetic intermediates to nanostructures. *Inorg. Chem.* 56, 8689–8697. doi: 10.1021/acs.inorgchem.7b00291
- Gaponenko, S., Demir, H. V., Seassal, C., and Woggon, U. (2016). Colloidal nanophotonics: the emerging technology platform. *Optics Express* 24, A430–A433. doi: 10.1364/OE.24.00A430
- Gary, D. C., Glassy, B. A., and Cossairt, B. M. (2014). Investigation of indium phosphide quantum dot nucleation and growth utilizing triarylsilylphosphine precursors. *Chem. Mater.* 26, 1734–1744. doi: 10.1021/cm500102q
- Gary, D. C., Terban, M. W., Billinge, S. J. L., and Cossairt, B. M. (2015). Two-step nucleation and growth of InP quantum dots via magic-sized cluster intermediates. *Chem. Mater.* 27, 1432–1441. doi: 10.1021/acs.chemmater.5b00286
- Green, M., and O'Brien, P. (1998). A novel metalorganic route for the direct and rapid synthesis of monodispersed quantum dots of indium phosphide. *Chem. Commun.* 22, 2459–2460. doi: 10.1039/a806419i
- Green, M., and O'Brien, P. (2001). A novel metalorganic route to nanocrystallites of zinc phosphide. *Chem. Mater.* 13, 4500–4505. doi: 10.1021/cm011009i
- Greenwood, N. N., Parish, R. V., and Thornton, P. (1966). Metal borides. *Q. Rev.* 20, 441–464. doi: 10.1039/qr9662000441
- Harris, D. K., and Bawendi, M. G. (2012). Improved precursor chemistry for the synthesis of III-V quantum dots. *J. Am. Chem. Soc.* 134, 20211–20213. doi: 10.1021/ja309863n
- Haubold, S., Haase, M., Kornowski, A., and Weller, H. (2001). Strongly luminescent InP/ZnS core-shell nanoparticles. *Chemphyschem* 2, 331–334. doi: 10.1002/1439-7641(20010518)2:5<331::AID-CPHC331>3.0.CO;2-0
- Henkes, A. E., and Schaak, R. E. (2007). Trioctylphosphine: a general phosphorus source for the low-temperature conversion of metals into metal phosphides. *Chem. Mater.* 19, 4234–4242. doi: 10.1021/cm071021w
- Ho, M. Q., Esteves, R. J. A., Kedarnath, G., and Arachchige, I. U. (2015). Size-dependent optical properties of luminescent Zn<sub>3</sub>P<sub>2</sub> quantum dots. *J. Phys. Chem. C* 119, 10576–10584. doi: 10.1021/acs.jpcc.5b01747
- Hong, G. S., Antaris, A. L., and Dai, H. J. (2017). Near-infrared fluorophores for biomedical imaging. *Nat. Biomed. Eng.* 1:0010. doi: 10.1038/s41551-016-0010
- Hunger, C., Ojo, W. S., Bauer, S., Xu, S., Zabel, M., Chaudret, B., et al. (2013). Stoichiometry-controlled FeP nanoparticles synthesized from a single source precursor. *Chem. Commun.* 49, 11788–11790. doi: 10.1039/c3cc46863a
- Imran, M., Caligiuri, V., Wang, M. J., Goldoni, L., Prato, M., Krahne, R., et al. (2018). Benzoyl halides as alternative precursors for the colloidal synthesis of lead-based halide perovskite nanocrystals. *J. Am. Chem. Soc.* 140, 2656–2664. doi: 10.1021/jacs.7b13477
- Jang, E. P., Jo, J. H., Lim, S. W., Lim, H. B., Kim, H. J., Han, C. Y., et al. (2018). Unconventional formation of dual-colored InP quantum dot-embedded silica composites for an operation-stable white light-emitting diode. *J. Mater. Chem. C* 6, 11749–11756. doi: 10.1039/C8TC04095H
- Janke, E. M., Williams, N. E., She, C. X., Zherebetsky, D., Hudson, M. H., Wang, L. L., et al. (2018). Origin of broad emission spectra in InP quantum dots: contributions from structural and electronic disorder. *J. Am. Chem. Soc.* 140, 15791–15803. doi: 10.1021/jacs.8b08753
- Joung, S., Yoon, S., Han, C. S., Kim, Y., and Jeong, S. (2012). Facile synthesis of uniform large-sized InP nanocrystal quantum dots using tris(tert-butyl(dimethylsilyl)phosphine). *Nanoscale Res. Lett.* 7:93. doi: 10.1186/1556-276X-7-93
- Jun, K. W., Khanna, P. K., Hong, K. B., Baeg, J. O., and Suh, Y. D. (2006). Synthesis of InP nanocrystals from indium chloride and sodium phosphide by solution route. *Mater. Chem. Phys.* 96, 494–497. doi: 10.1016/j.matchemphys.2005.07.041
- Kagan, C. R., Lifshitz, E., Sargent, E. H., and Talapin, D. V. (2016). Building devices from colloidal quantum dots. *Science* 353:aac5523. doi: 10.1126/science.aac5523
- Kang, H., Kim, S., Oh, J. H., Yoon, H. C., Jo, J. H., Yang, H., et al. (2018). Color-by-blue QD-emissive LCD enabled by replacing RGB color filters with narrow-band GR InP/ZnSeS/ZnS QD films. *Adv. Optic. Mater.* 6:1701239. doi: 10.1002/adom.201701239
- Keuleyan, S., Lhuillier, E., Brajuskovic, V., and Guyot-Sionnest, P. (2011). Mid-infrared HgTe colloidal quantum dot photodetectors. *Nat. Photo.* 5, 489–493. doi: 10.1038/nphoton.2011.142
- Khanna, P. K., Singh, N., and More, P. (2010). Synthesis and band-gap photoluminescence from cadmium phosphide nano-particles. *Curr. Appl. Phys.* 10, 84–88. doi: 10.1016/j.cap.2009.05.002
- Kim, K., Yoo, D., Choi, H., Tamang, S., Ko, J. H., Kim, S., et al. (2016). Halide-amine co-passivated indium phosphide colloidal quantum dots in tetrahedral shape. *Angew. Chem. Int. Ed. Engl.* 55, 3714–3718. doi: 10.1002/anie.201600289
- Kim, S., Kim, T., Kang, M., Kwak, S. K., Yoo, T. W., Park, L. S., et al. (2012). Highly luminescent InP/GaP/ZnS nanocrystals and their application to white light-emitting diodes. *J. Am. Chem. Soc.* 134, 3804–3809. doi: 10.1021/ja210211z
- Koh, S., Eom, T., Kim, W. D., Lee, K., Lee, D., Lee, Y. K., et al. (2017). Zinc-phosphorus complex working as an atomic valve for colloidal growth of monodisperse indium phosphide quantum dots. *Chem. Mater.* 29, 6346–6355. doi: 10.1021/acs.chemmater.7b01648
- Laufersky, G., Bradley, S., Frecaut, E., Lein, M., and Nann, T. (2018). Unraveling aminophosphine redox mechanisms for glovebox-free InP quantum dot syntheses. *Nanoscale* 10, 8752–8762. doi: 10.1039/C8NR01286E
- Lauth, J., Strupeit, T., Komowski, A., and Weller, H. (2013). A transmetalation route for colloidal GaAs nanocrystals and additional III-V semiconductor materials. *Chem. Mater.* 25, 1377–1383. doi: 10.1021/cm3019617
- Li, D. Z., Peng, L. C., Zhang, Z. L., Shi, Z., Xie, R. G., Han, M. Y., et al. (2014). Large scale synthesis of air stable precursors for the preparation of high quality metal arsenide and phosphide nanocrystals as efficient emitters covering the visible to near infrared region. *Chem. Mater.* 26, 3599–3602. doi: 10.1021/cm500581m
- Li, L., Protiere, M., and Reiss, P. (2008). Economic synthesis of high quality InP nanocrystals using calcium phosphide as the phosphorus precursor. *Chem. Mater.* 20, 2621–2623. doi: 10.1021/cm7035579
- Li, L., and Reiss, P. (2008). One-pot synthesis of highly luminescent InP/ZnS nanocrystals without precursor injection. *J. Am. Chem. Soc.* 130, 11588–11589. doi: 10.1021/ja803687e
- Lim, J., Bae, W. K., Lee, D., Nam, M. K., Jung, J., Lee, C., et al. (2011). InP@ZnSeS<sub>x</sub> core@composition gradient shell quantum dots with enhanced stability. *Chem. Mater.* 23, 4459–4463. doi: 10.1021/cm201550w
- Lim, J., Park, M., Bae, W. K., Lee, D., Lee, S., Lee, C., et al. (2013). Highly efficient cadmium-free quantum dot light-emitting diodes enabled by the direct formation of excitons within InP@ZnSeS quantum dots. *ACS Nano* 7, 9019–9026. doi: 10.1021/nn403594j
- Lin, G. M., Ouyang, Q. L., Hu, R., Ding, Z. C., Tian, J. L., Yin, F., et al. (2015). *In vivo* toxicity assessment of non-cadmium quantum dots in BALB/c mice. *Nanomed. Nanotechnol. Biol. Med.* 11, 341–350. doi: 10.1016/j.nano.2014.10.002
- Liu, J. F., Meyns, M., Zhang, T., Arbiol, J., Cabot, A., and Shavel, A. (2018). Triphenyl phosphite as the phosphorus source for the scalable and cost-effective production of transition metal phosphides. *Chem. Mater.* 30, 1799–1807. doi: 10.1021/acs.chemmater.8b00290
- Liu, Z. K., Mu, H. R., Xiao, S., Wang, R. B., Wang, Z. T., Wang, W. W., et al. (2016). Pulsed lasers employing solution-processed plasmonic Cu<sub>3</sub>xP colloidal nanocrystals. *Adv. Mater.* 28, 3535–3542. doi: 10.1002/adma.201504927
- Liu, Z. P., Kumbhar, A., Xu, D., Zhang, J., Sun, Z. Y., and Fang, J. Y. (2008). Coreduction colloidal synthesis of III-V nanocrystals: the case of InP. *Angew. Chem. Int. Edn.* 47, 3540–3542. doi: 10.1002/anie.200800281
- Luber, E. J., Mobarok, M. H., and Buriak, J. M. (2013). Solution-processed zinc phosphide ( $\alpha$ -Zn<sub>3</sub>P<sub>2</sub>) colloidal semiconductor nanocrystals for thin film photovoltaic applications. *ACS Nano* 7, 8136–8146. doi: 10.1021/nn4034234

- Manna, G., Bose, R., and Pradhan, N. (2013). Semiconducting and plasmonic copper phosphide platelets. *Angew. Chem. Int. Edn.* 52, 6762–6766. doi: 10.1002/anie.201210277
- Miao, S., Yang, T., Hickey, S. G., Lesnyak, V., Rellinghaus, B., Xu, J. Z., et al. (2013). Emissive ZnO@Zn3P2 nanocrystals: synthesis, optical, and optoelectrochemical properties. *Small* 9, 3415–3422. doi: 10.1002/sml.201203023
- Miao, S. D., Hickey, S. G., Rellinghaus, B., Waurisch, C., and Eychmuller, A. (2010). Synthesis and characterization of cadmium phosphide quantum dots emitting in the visible red to near-infrared. *J. Am. Chem. Soc.* 132, 5613–5615. doi: 10.1021/ja9105732
- Miao, S. D., Hickey, S. G., Waurisch, C., Lesnyak, V., Otto, T., Rellinghaus, B., et al. (2012). Synthesis of monodisperse cadmium phosphide nanoparticles using *ex-situ* produced phosphine. *ACS Nano* 6, 7059–7065. doi: 10.1021/nn3021037
- Michalet, X., Pinaud, F. F., Bentolila, L. A., Tsay, J. M., Doose, S., Li, J. J., et al. (2005). Quantum dots for live cells, *in vivo* imaging, and diagnostics. *Science* 307, 538–544. doi: 10.1126/science.1104274
- Micic, O. I., Cheong, H. M., Fu, H., Zunger, A., Sprague, J. R., Mascarenhas, A., et al. (1997). Size-dependent spectroscopy of InP quantum dots. *J. Phys. Chem. B* 101, 4904–4912. doi: 10.1021/jp9704731
- Micic, O. I., Curtis, C. J., Jones, K. M., Sprague, J. R., and Nozik, A. J. (1994). Synthesis and characterization of InP quantum dots. *J. Phys. Chem.* 98, 4966–4969. doi: 10.1021/j100070a004
- Micic, O. I., Sprague, J., Lu, Z. H., and Nozik, A. J. (1996). Highly efficient band-edge emission from InP quantum dots. *Appl. Phys. Lett.* 68, 3150–3152.
- Micic, O. I., Sprague, J. R., Curtis, C. J., Jones, K. M., Machol, J. L., Nozik, A. J., et al. (1995). Synthesis and characterization of InP, GaP, and GaInP2 quantum dots. *J. Phys. Chem.* 99, 7754–7759.
- Mobarok, M. H., Lubber, E. J., Bernard, G. M., Peng, L., Wasylshen, R. E., and Buriak, J. M. (2014). Phase-pure crystalline zinc phosphide nanoparticles: synthetic approaches and characterization. *Chem. Mater.* 26, 1925–1935. doi: 10.1021/cm500557f
- Mundy, M. E., Ung, D., Lai, N. L., Jahrman, E. P., Seidler, G. T., and Cossairt, B. M. (2018). Aminophosphines as versatile precursors for the synthesis of metal phosphide nanocrystals. *Chem. Mater.* 30, 5373–5379. doi: 10.1021/acs.chemmater.8b02206
- Nedelcu, G., Protesescu, L., Yakunin, S., Bodnarchuk, M. I., Grotevent, M. J., and Kovalenko, M. V. (2015). Fast anion-exchange in highly luminescent nanocrystals of cesium lead halide perovskites (CsPbX<sub>3</sub>, X = Cl, Br, I). *Nano Lett.* 15, 5635–5640. doi: 10.1021/acs.nanolett.5b02404
- Ojo, W. S., Xu, S., Delpach, F., Nayral, C., and Chaudret, B. (2012). Room-temperature synthesis of air-stable and size-tunable luminescent ZnS-coated Cd3P2 nanocrystals with high quantum yields. *Angew. Chem. Int. Edn.* 51, 738–741. doi: 10.1002/anie.201104864
- Panfil, Y. E., Oded, M., and Banin, U. (2018). Colloidal quantum nanostructures: emerging materials for display applications. *Angew. Chem. Int. Edn.* 57, 4274–4295. doi: 10.1002/anie.201708510
- Park, J., Koo, B., Yoon, K. Y., Hwang, Y., Kang, M., Park, J. G., et al. (2005). Generalized synthesis of metal phosphide nanorods via thermal decomposition of continuously delivered metal-phosphine complexes using a syringe pump. *J. Am. Chem. Soc.* 127, 8433–8440. doi: 10.1021/ja0427496
- Perera, S. C., Fodor, P. S., Tsoi, G. M., Wenger, L. E., and Brock, S. L. (2003). Application of de-silylation strategies to the preparation of transition metal pnictide nanocrystals: the case of FeP. *Chem. Mater.* 15, 4034–4038. doi: 10.1021/cm034443o
- Pietra, F., De Trizio, L., Hoekstra, A. W., Renaud, N., Prato, M., Grozema, F. C., et al. (2016). Tuning the lattice parameter of InxZnyP for highly luminescent lattice-matched core/shell quantum dots. *ACS Nano* 10, 4754–4762. doi: 10.1021/acsnano.6b01266
- Pietra, F., Kirkwood, N., De Trizio, L., Hoekstra, A. W., Kleibergen, L., Renaud, N., et al. (2017). Ga for Zn cation exchange allows for highly luminescent and photostable InZnP-based quantum dots. *Chem. Mater.* 29, 5192–5199. doi: 10.1021/acs.chemmater.7b00848
- Pietryga, J. M., Park, Y. S., Lim, J. H., Fidler, A. F., Bae, W. K., Brovelli, S., et al. (2016). Spectroscopic and device aspects of nanocrystal quantum dots. *Chem. Rev.* 116, 10513–10622. doi: 10.1021/acs.chemrev.6b00169
- Pu, C., Qin, H., Gao, Y., Zhou, J., Wang, P., and Peng, X. (2017). Synthetic control of exciton behavior in colloidal quantum dots. *J. Am. Chem. Soc.* 139, 3302–3311. doi: 10.1021/jacs.6b11431
- Qian, L., Zheng, Y., Xue, J. G., and Holloway, P. H. (2011). Stable and efficient quantum-dot light-emitting diodes based on solution-processed multilayer structures. *Nat. Photo.* 5, 543–548. doi: 10.1038/nphoton.2011.171
- Rafipour, M., Dupont, D., Tornatzky, H., Tessier, M. D., Maultzsch, J., Hens, Z., et al. (2018). Strain engineering in InP/(Zn,Cd)Se core/shell quantum dots. *Chem. Mater.* 30, 4393–4400. doi: 10.1021/acs.chemmater.8b01789
- Ramasamy, P., Kim, N., Kang, Y. S., Ramirez, O., and Lee, J. S. (2017). Tunable, bright, and narrow-band luminescence from colloidal indium phosphide quantum dots. *Chem. Mater.* 29, 6893–6899. doi: 10.1021/acs.chemmater.7b02204
- Ramasamy, P., Ko, K. J., Kang, J. W., and Lee, J. S. (2018). Two-step “seed-mediated” synthetic approach to colloidal indium phosphide quantum dots with high-purity photo- and electroluminescence. *Chem. Mater.* 30, 3643–3647. doi: 10.1021/acs.chemmater.8b02049
- Reiss, P., Carriere, M., Linceneau, C., Vaure, L., and Tamang, S. (2016). Synthesis of semiconductor nanocrystals, focusing on nontoxic and earth-abundant materials. *Chem. Rev.* 116, 10731–10819. doi: 10.1021/acs.chemrev.6b00116
- Sahu, A., Kang, M. S., Kompch, A., Notthoff, C., Wills, A. W., Deng, D., et al. (2012). Electronic impurity doping in CdSe nanocrystals. *Nano Lett.* 12, 2587–2594. doi: 10.1021/nl300880g
- Shen, W., Tang, H. Y., Yang, X. L., Cao, Z. L., Cheng, T., Wang, X. Y., et al. (2017). Synthesis of highly fluorescent InP/ZnS small-core/thick-shell tetrahedral-shaped quantum dots for blue light-emitting diodes. *J. Mater. Chem. C* 5, 8243–8249. doi: 10.1039/C7TC02927F
- Song, W. S., Lee, H. S., Lee, J. C., Jang, D. S., Choi, Y., Choi, M., et al. (2013). Amine-derived synthetic approach to color-tunable InP/ZnS quantum dots with high fluorescent qualities. *J. Nanopart. Res.* 15:1750. doi: 10.1007/s11051-013-1750-y
- Steckel, J. S., Coe-Sullivan, S., Bulovic, V., and Bawendi, M. G. (2003). 1.3 μm to 1.55 μm tunable electroluminescence from PbSe quantum dots embedded within an organic device. *Adv. Mater.* 15, 1862–1866. doi: 10.1002/adma.200305449
- Sun, T., Wang, Y. J., Yu, W. Z., Wang, Y. S., Dai, Z. G., Liu, Z. K., et al. (2017). Flexible broadband graphene photodetectors enhanced by plasmonic Cu<sub>3</sub>xP colloidal nanocrystals. *Small* 13:1701881. doi: 10.1002/sml.201701881
- Talapin, D. V., Lee, J. S., Kovalenko, M. V., and Shevchenko, E. V. (2010). Prospects of colloidal nanocrystals for electronic and optoelectronic applications. *Chem. Rev.* 110, 389–458. doi: 10.1021/cr900137k
- Tamang, S., Linceneau, C., Hermans, Y., Jeong, S., and Reiss, P. (2016). Chemistry of InP nanocrystal syntheses. *Chem. Mater.* 28, 2491–2506. doi: 10.1021/acs.chemmater.5b05044
- Tessier, M. D., Baquero, E. A., Dupont, D., Grigel, V., Bladt, E., Bals, S., et al. (2018). Interfacial oxidation and photoluminescence of InP-based core/shell quantum dots. *Chem. Mater.* 30, 6877–6883. doi: 10.1021/acs.chemmater.8b03117
- Tessier, M. D., De Nolf, K., Dupont, D., Sinnaeve, D., De Roo, J., and Hens, Z. (2016). Aminophosphines: a double role in the synthesis of colloidal indium phosphide quantum dots. *J. Am. Chem. Soc.* 138, 5923–5929. doi: 10.1021/jacs.6b01254
- Tessier, M. D., Dupont, D., De Nolf, K., De Roo, J., and Hens, Z. (2015). Economic and size-tunable synthesis of InP/ZnE (E = S, Se) colloidal quantum dots. *Chem. Mater.* 27, 4893–4898. doi: 10.1021/acs.chemmater.5b02138
- Ung, T. D. T., Tran, T. T. H., Nguyen, Q. L., and Reiss, P. (2008). Low temperature synthesis of InP nanocrystals. *Mater. Chem. Phys.* 112, 1120–1123. doi: 10.1016/j.matchemphys.2008.07.051
- Vinokurov, A., Chernysheva, G., Mordvinova, N., and Dorofeev, S. (2018). Optical properties and structure of Ag-doped InP quantum dots prepared by a phosphine synthetic route. *Dalton Trans.* 47, 12414–12419. doi: 10.1039/C8DT02434K
- Wang, H. C., Zhang, H., Chen, H. Y., Yeh, H. C., Tseng, M. R., Chung, R. J., et al. (2017). Cadmium-free InP/ZnSeS/ZnS heterostructure-based quantum dot light-emitting diodes with a ZnMgO electron transport layer and a brightness of over 10 000 cd m<sup>-2</sup>. *Small* 13:1603962. doi: 10.1002/sml.201603962
- Xie, R., Battaglia, D., and Peng, X. G. (2007). Colloidal InP nanocrystals as efficient emitters covering blue to near-infrared. *J. Am. Chem. Soc.* 129, 15432–15433. doi: 10.1021/ja076363h

- Xie, R. G., Zhang, J. X., Zhao, F., Yang, W. S., and Peng, X. G. (2010). Synthesis of monodisperse, highly emissive, and size-tunable Cd<sub>3</sub>P<sub>2</sub> nanocrystals. *Chem. Mater.* 22, 3820–3822. doi: 10.1021/cm1008653
- Yang, W., He, G. X., Mei, S. L., Zhu, J. T., Zhang, W. L., Chen, Q. H., et al. (2017). Controllable synthesis of dual emissive Ag:InP/ZnS quantum dots with high fluorescence quantum yield. *Appl. Surf. Sci.* 423, 686–694. doi: 10.1016/j.apsusc.2017.06.048
- Yang, X., Zhao, D. W., Leck, K. S., Tan, S. T., Tang, Y. X., Zhao, J. L., et al. (2012). Full visible range covering InP/ZnS nanocrystals with high photometric performance and their application to white quantum dot light-emitting diodes. *Adv. Mater.* 24, 4180–4185. doi: 10.1002/adma.201104990
- Zan, F., and Ren, J. C. (2012). Gas-liquid phase synthesis of highly luminescent InP/ZnS core/shell quantum dots using zinc phosphide as a new phosphorus source. *J. Mater. Chem.* 22, 1794–1799. doi: 10.1039/C1JM13982G
- Zhang, A. D., Dong, C. Q., Liu, H., and Ren, J. C. (2013). Blinking behavior of CdSe/CdS quantum dots controlled by alkylthiols as surface trap modifiers. *J. Phys. Chem. C* 117, 24592–24600. doi: 10.1021/jp408544x
- Zhang, Z. L., Liu, D., Li, D. Z., Huang, K. K., Zhang, Y., Shi, Z., et al. (2015). Dual emissive Cu:InP/ZnS/InP/ZnS nanocrystals: single-source “greener” emitters with flexibly tunable emission from visible to near-infrared and their application in white light-emitting diodes. *Chem. Mater.* 27, 1405–1411. doi: 10.1021/cm5047269
- Ziegler, J., Xu, S., Kucur, E., Meister, F., Batentschuk, M., Gindele, F., et al. (2008). Silica-coated InP/ZnS nanocrystals as converter material in white LEDs. *Adv. Mater.* 20, 4068–4073. doi: 10.1002/adma.200800724

**Conflict of Interest Statement:** The authors declare that the research was conducted in the absence of any commercial or financial relationships that could be construed as a potential conflict of interest.

Copyright © 2019 Li, Jia, Meng and Li. This is an open-access article distributed under the terms of the Creative Commons Attribution License (CC BY). The use, distribution or reproduction in other forums is permitted, provided the original author(s) and the copyright owner(s) are credited and that the original publication in this journal is cited, in accordance with accepted academic practice. No use, distribution or reproduction is permitted which does not comply with these terms.